

Interlayer and moiré excitons in atomically thin double layers: from individual quantum emitters to degenerate ensembles

Mauro Brotons-Gisbert,^{1,*} Brian D. Gerardot,^{1,†} Alexander W. Holleitner,^{2,‡} and Ursula Wurstbauer^{3,§}

¹*Institute of Photonics and Quantum Sciences, SUPA, Heriot-Watt University, Edinburgh EH14 4AS, UK*

²*Walter Schottky Institute and Physics Department, Technical*

University of Munich, Am Coulombwall 4a, 85748 Garching, Germany

³*Institute of Physics, University of Münster, Wilhelm-Klemm-Str. 10, 48149 Münster, Germany*

(Dated: July 16, 2024)

Interlayer excitons (IXs), composed of electron and hole states localized in different layers, excel in bilayers composed of atomically thin van der Waals materials such as semiconducting transition metal dichalcogenides (TMDs) due to drastically enlarged exciton binding energies, exciting spin-valley properties, elongated lifetimes, and large permanent dipoles. The latter allows modification by electric fields and the study of thermalized bosonic quasiparticles, from the single particle level to interacting degenerate dense ensembles. Additionally, the freedom to combine bilayers of different van der Waals materials without lattice or relative twist angle constraints leads to layer hybridized and moiré excitons which can be widely engineered. This review covers fundamental aspects of IXs including correlation phenomena as well as the consequence of moiré superlattices with a strong focus on TMD homo- and hetero-bilayers.

Keywords: 2D materials, transition metal dichalcogenides, semiconductor optics, van der Waals hetero-structures, moiré crystals, excitons, dipolar interactions

INTRODUCTION

Van der Waals (vdW) bilayers host a plethora of different exciton species with different properties and functionalities that are promising for applications. Vice versa, excitons can serve as sensitive probes for the local potential landscape in vdW hetero-structures. Such vdW stacks can be prepared from the same or different two-dimensional crystals and are called homo-bilayer or hetero-bilayer, respectively. As Coulomb-bound electron-hole pairs, excitons are very sensitive to their dielectric environment inside and outside of the semiconducting host materials. Moreover, the excitonic properties strongly depend on the underlying Bloch states. Like in two-dimensional monolayers, a reduced dielectric screening and the two-dimensional nature of the bilayers results in excitonic binding energies exceeding several hundreds of millielectron volts. Unlike monolayers, vertical vdW double layers can host excitons with the constituting electron and hole states being localized in adjacent layers. As a direct consequence, the reduced overlap of the electron – hole wavefunctions results in enhanced lifetimes, up to several 100s of nanoseconds [1, 2], allowing the study of thermalized ensembles [3] of such interlayer excitons (IXs). Another peculiarity of IXs is their permanent dipole moment, which enables one to tune their energy and to control them by electric fields in capacitor structures [4] that can be realized even in devices prepared only from vdW materials with e.g. hBN as a dielectric material and graphene or thin graphite as semi-transparent electrodes. In addition to manipulating the IX energy, momentum-dependent hybridization of the IXs with other exciton species (in particular intralayer excitons with strong oscillator strengths) can

be controlled by external stimuli such as electric fields [5, 6], pressure [7, 8], or twist angle [9]. In this way, the competition and coupling between intralayer, interlayer and layer-hybridized excitons emitting at the fundamental gap as well as from higher lying states can be experimentally accessed [10]. While also lateral vdW hetero-structures can host IXs [11], this review focuses on the peculiarities of excitons in vertical vdW bilayers prepared from semiconducting transition metal dichalcogenide (TMD) monolayers. With several engineering opportunities, TMD-based vdW stacks hold fascinating properties that individual layers or conventional 3D solids typically do not exhibit within one material: (i) depending on the material combination, rich IX physics can be addressed including the dynamics of neutral, charged, and layer-hybridized IXs, as well as layer-specific characteristics of higher-lying IXs. (ii) Stacking of two lattices with similar but not identical lattice constants and/or a relative twist angle results in the formation of a moiré lattice. A moiré lattice is a geometrical superimposed periodic patterns that forms by stacking two atomically thin commensurate with a relative twist angle, or two crystals with different lattice constants or both together. The long-period moiré super-lattice structure causes highly periodic potential modulations in real space [12] and flat moiré minibands in the reciprocal space for specific lattice mismatches and twist angles [13]. The zero-dimensional potential traps can host so-called moiré excitons that can function as single photon emitters allowing for the creation of periodic networks of quantum emitters [14, 15]. Similar to magic angle twisted bilayer graphene [16], in twisted bilayer TMDs, strongly correlated states can emerge by the combination of a quenched kinetic energy and a high density of states in the flat minibands,

which can act as sensitive probes for correlated phases of adjacent charge carrier systems [13, 17–20]. Compared to intralayer excitons, IXs exhibit superior sensitivity due to their permanent dipolar moment [21]. In hetero-bilayers of TMDs, excitons can not only sense correlated states, but also correlated excitonic states, such as an excitonic insulator, can emerge [22–24]. Moreover, the presence of strong spin-orbit coupling gives rise to even more exotic correlated states [25]. This high degree of tunability of rich exciton physics makes vertical vdW double layers a highly interesting research subject for fundamental studies on both many-body and correlation phenomena of low-dimensional exciton and charge carrier systems. On a more applied perspective, such highly tunable characteristics suggest various possibilities of optoelectronic and quantum photonic devices such as solar cells, light emitting diodes, photo-sensors or single-photon sources operating in a largely extended spectral range covering the near-infrared to ultraviolet wavelength ranges. This review article is organized as follows: After this introduction and a brief summary on the most fundamental properties of TMD semiconductors, IXs and dipolar excitons are discussed, followed by an introduction of excitons in TMD moiré hetero-structures and hybridization of intra- and interlayer excitons as well as the impact of structural effects. Next, interaction effects, including the formation of degenerate IX ensembles, are considered, followed by a discussion of IX formation and transport processes. The article concludes with a brief summary and an outlook.

BACKGROUND

Two-dimensional group-VI TMD semiconductors of the form MX_2 (with $\text{M} = \text{Mo}, \text{W}$, and $\text{X} = \text{S}, \text{Se}$) have attracted much attention due to their appealing properties for a large palette of optoelectronics, spintronics, and photonics applications. The investigation of their structural, electronic, and optical properties constitutes a very active research field in the solid-state and photonics communities. Consequently, the main properties of 2D TMD semiconductors are extensively covered and reviewed in the literature for both their bulk and few layers forms [26, 27]. Among their main properties, TMDs monolayers are well known by their momentum-direct optical band gaps with energies in the visible to near-infrared spectral range, with the band edges located at the degenerate but inequivalent corners of the Brillouin zone (typically referred to as $\pm\text{K}$ valleys). Carriers occupying the conduction and valence band edges at $\pm\text{K}$ form excitons that are hydrogen-like states with a typical binding energy on the order of 0.5 eV [28, 29]. Due to their large binding energy, excitons dominate the optical response of TMDs at both cryogenic and room temperatures. Moreover, the strong spin-orbit coupling induced by the heavy transition-metal atoms and the broken in-

version symmetry of the TMDs lattice unit cell lead to an effective coupling between the valley index and spin of the electrons and holes at the $\pm\text{K}$ corners [30]. This effective coupling (typically referred to as spin-valley locking), results in valley-dependent optical selection rules [31]: excitonic absorption and emission processes at $\pm\text{K}$ involve σ^\pm -polarized photons, respectively, enabling optical control of excitons [32, 33].

INTERLAYER EXCITONS AND DIPOLES

Interlayer excitons in natural multi-layer TMDs

Despite their indirect-gap nature, multi-layer TMDs preserve the direct gap at the $\pm\text{K}$ corners of the Brillouin zone even in the bulk limit, with spin-orbit-split conduction bands that present a flat dispersion along the out-of-plane direction (i.e., the K-H high-symmetry direction) [7, 34]. Such flat band dispersion ensures that the electron wave functions around $\pm\text{K}$ are highly confined within each individual layer, resulting in the formation of intralayer excitons, i.e. excitons in which the electron-hole pairs are localized in the same layer (see Figure 1A). In addition to intralayer excitons, the layer-localized electron wave functions in TMD multi-layers can also bind to holes with wave functions confined within adjacent layers or that spread along several layers, giving rise to IXs with spatially displaced wave functions [34–39]. Interlayer and intralayer excitons coexist in multi-layer TMDs (see Figure 1A, top [40]), with both exciton species depicting momentum-direct optical transitions at $\pm\text{K}$. The bottom panel of figure 1A shows a schematic of the spin, band and layer configurations of dipole-allowed intralayer and IXs for bilayer $2H\text{-MoS}_2$, a prototypical centrosymmetric multi-layer TMD. Ground-state intralayer excitons (the so called A excitons) show optical transitions involving an electron in the lowest conduction band and a hole in the highest valence band (red arrows), while intralayer B excitons present optical transitions between the topmost spin-orbit-split conduction band and the lower spin-orbit-split valence band at $\pm\text{K}$ (blue arrows). Dipole allowed IXs present optical transitions between the topmost valence band in one layer and the upper spin-orbit-split conduction band in the other layer (green arrows). Consequently, dipole-allowed interlayer and intralayer excitons exhibit optical transitions with similar symmetry properties, with the difference that the spin-valley selectivity characteristic of monolayer TMDs is replaced by a spin-layer selectivity in the optical generation of excitons with circular polarized light. As detailed below, stacking-order dependent hybridization can give rise to a hole state that is delocalized across different layers [40, 41].

Figure 1B shows differential reflectance spectra (DR/R) of monolayer, bilayer and trilayer $2H\text{-MoS}_2$ samples (black, red and blue solid lines, respectively) for a

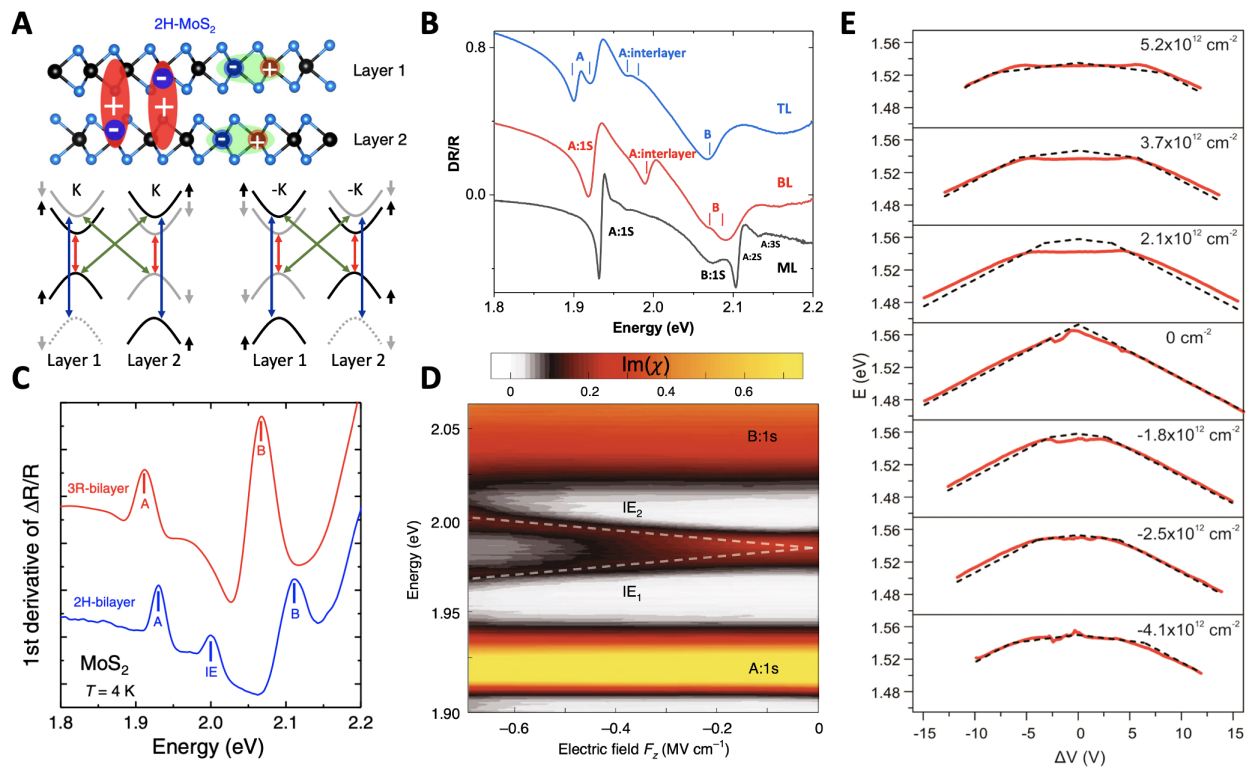


FIG. 1. Interlayer excitons in homobilayer TMDs [MoS₂ (A-D) and WSe₂ (E)].

(A) Top: schematics showing the intralayer and interlayer nature of the excitons in bilayer 2H-MoS₂. Bottom: sketch of the spin, valley and layer configuration of the optical transitions corresponding to intralayer A excitons (red arrows), intralayer B excitons (blue arrows), and IXs (green arrows) in bilayer 2H-MoS₂. (B) Differential reflectivity of ML, BL and TL 2H-MoS₂ (black, red and blue solid lines, respectively) for a sample temperature of $T = 4$ K. (C) First derivative of the differential reflectivity spectrum for as-grown 2H-bilayer (blue) and as-grown 3R-bilayer (red) MoS₂ 4 K. (D) Color map of the absorption spectra of bilayer MoS₂ showing a Stark shift of the IXs at small electric fields. The intralayer A:1s and B:1s and the two branches of the IX resonances (IE₁ and IE₂) are labelled. (E) IX emission energy in BL WSe₂ as a function of the applied electric field for different electron doping densities. Adapted with permission from Ref. [40], Nature Publishing Group (A, C), Ref. [42], APS (B), Ref. [37], Nature Publishing Group (B), and Ref. [35], ACS (E).

sample temperature of $T = 4$ K [42], in which an absorption peak arising from IXs can be seen for the bilayer and trilayer samples. Despite the large spatial separation of the electron and hole wavefunctions, IXs in multi-layer TMDs possess binding energies almost an order of magnitude larger compared with those in coupled III-V quantum wells, and of the same order of magnitude as their intralayer counterparts [42]. Consequently, the optical transitions associated to IXs in TMDs can appear either at lower or at higher energies than the intralayer A exciton depending on the dark or bright nature of the ground IX state, respectively. Interestingly, the stacking order of the TMD multilayers has a strong impact on the formation of IXs. In Ref. [40], the authors demonstrated that hole delocalization over MoS₂ homo-bilayers is allowed for 2H stacking but forbidden for 3R stacking, resulting in the presence (absence) of IXs in 2H-MoS₂ (3R-MoS₂) homo-bilayers (see Figure 1C [40]). However, a more recent work showed the presence of IXs in R-MoS₂ bilayers

depicting an asymmetric interlayer coupling arising from a layer-dependent Berry phase effect. Such an asymmetric coupling is also the electronic origin of spontaneous polarization characteristic of R-stacked TMDs [41].

Moreover, the spatial displacement of the exciton carriers in TMD homo-bilayers endows IXs with a large out-of-plane static electric dipole that can be tuned via the Stark effect [37–39]. Figure 1D depicts a color map of the absorption spectra of bilayer 2H-MoS₂ showing a Stark shift of the IXs for applied vertical electric fields [37]. Here, the IX resonance splits into two branches (IE₁ and IE₂) that shift linearly to lower (higher) energy depending on the parallel (anti-parallel) orientation of the electric field and the permanent electric dipole. The effects of an applied vertical electric field on the IX resonance energy and its recombination dynamics have also been investigated in dual-gated homo-bilayer WSe₂ and MoSe₂ devices [35, 43]. Via photoluminescence (PL) and time-resolved PL spectroscopy at 10 K, the authors in Ref.

[35] show that the IX emission redshifts symmetrically for both positive and negative applied vertical electric fields. The symmetrical redshift of the exciton energy for both positive and negative fields is attributed to the electric-field-induced redistribution of carriers among the two layers that results in a parallel alignment of the exciton permanent dipole with the applied field. Figure 1E summarizes the Stark shift observed under different doping densities (positive values n for electron doping and negative values for hole doping) [35]. Close to the charge neutrality point, a linear Stark effect emerges immediately, whereas for finite electron or hole doping densities an appreciable Stark effect is observed only for applied gate voltages beyond a threshold value. The existence of a threshold gate voltage can be understood as an offset in the resulting electric field produced by an unequal distribution of carriers between the two layers as a consequence of the applied field [35]. Beyond natural bilayer TMD systems, ground and excited-state IXs with large permanent dipole moments were also been reported in trilayer 2H-MoSe₂ and three-, four-, five-, and seven-layer 2H-WSe₂, in which the wavefunctions of the carriers forming the excitons are confined in an every-other-layer configuration [43, 44]. Finally, in addition to the Stark effect, the application of vertical electric fields can result in an enhancement of the IX recombination lifetime by more than two orders of magnitude [35].

Excitons in TMD moiré hetero-structures

In contrast to TMD homo-bilayers, stacking any two different ML TMDs creates a hetero-bilayer typically with type-II band alignment while preserving atomically sharp interfaces [45–47]. Such a band alignment results in the formation of IXs with smaller transition energies than the intralayer excitons in the individual monolayers, from which the IXs localized at the $\pm K$ valleys inherit their valley-contrasting physics [4, 48–50], although indirect IXs with an inter-valley nature also arise in many combinations of homo- and hetero-bilayers [51]. In addition, the interlayer nature of the excitons leads to a reduced overlap of the electron and hole wave functions, which results in optical dipole transitions with long radiative lifetimes compared to intralayer excitons [48, 51, 52]. Similar to IXs in TMD homo-bilayers, the separation of the exciton carriers can result in a large permanent electric out-of-plane dipole moment that enables a large tunability of the exciton transition energy by vertically applied electric fields [4, 14, 53]. Moreover, similar to monolayer TMDs [54, 55], patterned substrates were shown to lead to local strain profiles that enable exciton trapping in nanoscale confinement potentials, in which the mean number of trapped IXs can be controlled via the optical excitation level [56, 57].

Single interlayer exciton moiré trapping

Beyond the large permanent dipole moment and the spin-valley physics, the compelling concept of a moiré superlattice emerges in TMD hetero-bilayers with lattice mismatch and/or any relative twist angle between the constituent monolayers [12]. The moiré superlattice creates a periodic potential landscape for IXs [58–60], in which three high-symmetry sites (A, B, and C) with specific atomic registries arise, such as R_h^h (A), R_h^X (B) and R_h^M (C), where R_h^μ denotes an R-type stacking with the μ site of the electron layer (either h the hexagon centre, X the chalcogen site or M the metal site) vertically aligned with the hexagon centre (h) of the hole layer (Figure 2A). For moiré periods larger than the IX Bohr radius that is in the order of a few nanometers [61], these moiré high-symmetry sites can behave as smooth quantum-dot-like confining potentials, leading to the trapping of single electrons, holes, or IXs [58, 59]. The moiré potential minima preserve the three-fold rotational (C_3) symmetry [58, 59], and excitons trapped in such moiré sites obey selection rules that depend on the spin configuration of the exciton carriers (spin-singlet/spin-triplet) and the atomic registry of the trapping site, as theoretically predicted (see Figure 2A) [62]. Experimental evidence of neutral IXs trapped in a moiré potential has been reported in MoSe₂/WSe₂ hetero-bilayers with twist angles of around 0°, 21.8° and 60° at cryogenic temperatures [14, 63–65]. Hetero-bilayers with twist angles of around 0° present ground IX states with spin-singlet configurations, while hetero-bilayers with twist angles of 21.8° and 60° present ground exciton states with spin-triplet optical transitions. For small IX densities, polarization-resolved PL measurements show that the moiré-trapped IXs exhibit linewidths below 100 μeV with strong helical polarization due to the C_3 symmetry, which results in a notable absence of observable fine structure [14, 63, 64] (Figure 2B, top). Moreover, the trapped IXs show well-defined magneto-optical properties: The g factors of the trapped excitons depend on the relative valley alignment (i.e., stacking configuration) between the layers hosting the carriers (Figure 2B, bottom) [14, 63, 64]. In addition, the emission from the localized interlayer excitons presents clear hallmarks of quantum-confined excitons: power-dependent emission intensities that can be described by a two-level saturation model [14, 63, 64] and photon antibunching (Figure 2C) [14]. Finally, the large permanent dipole of the moiré-trapped IXs can be exploited to achieve large direct current Stark tuning of their emission energies up to 40 meV [14].

Moiré interlayer trions

In addition to neutral IXs, the loading of additional charge carriers into the moiré lattice in gate-tunable

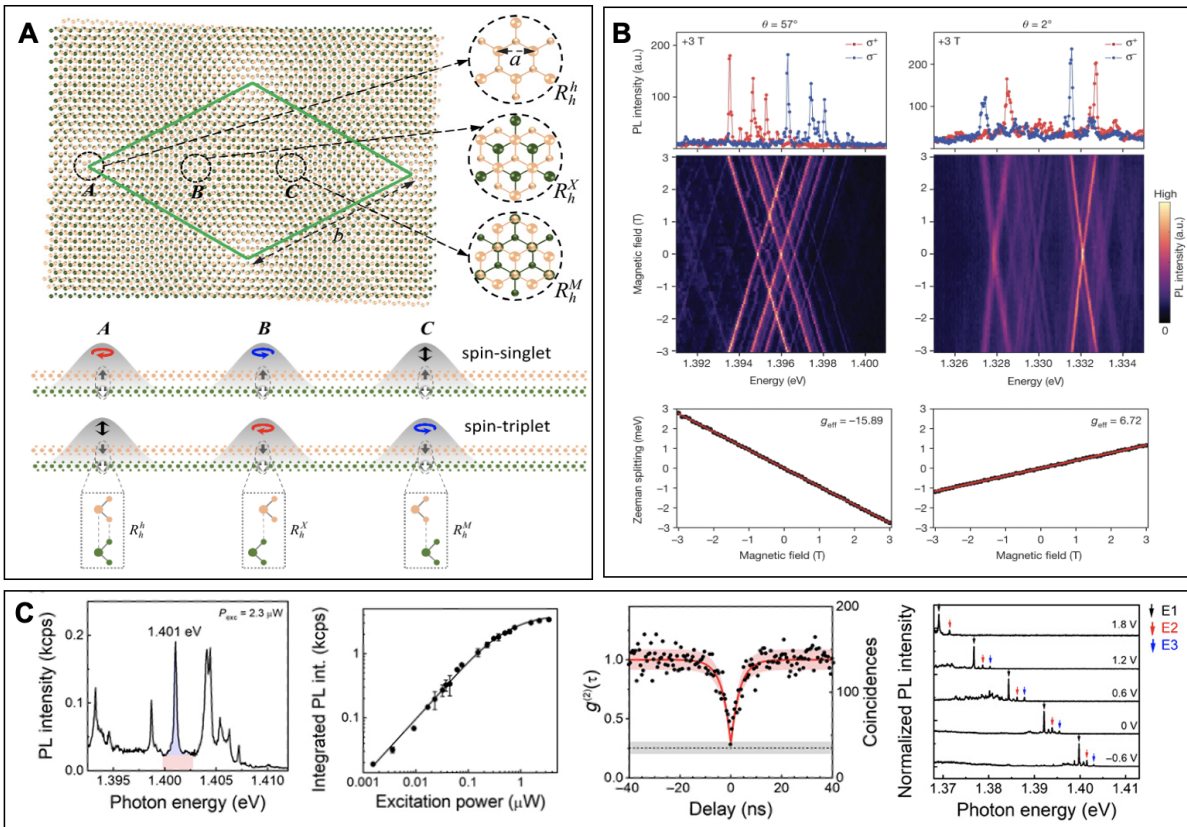


FIG. 2. Moiré-trapped IXs in MoSe₂/WSe₂ hetero-bilayers [MX₂/WX₂ (A) and MoSe₂/WSe₂ (B, C)].

(A) Top: schematics of the long-period moiré pattern in a R-stacked MoX₂/WX₂ hetero-bilayer. Green diamond denotes the moiré supercell. Insets show zooms of the local atomic registries in the three high-symmetry trapping sites (A, B and C) of the moiré supercell. A, B and C have atomic registries R_h^h , R_h^X and R_h^M , respectively. Bottom: schematic illustration of the polarization selection rules, for K-valley spin-singlet and spin-triplet IX wavepackets centered at trapping sites A, B and C, respectively. (B) Helicity-resolved PL of moiré-trapped IXs in MoSe₂/WSe₂ hetero-bilayers with twist angles of 57° (left) and 2° (right) as a function of the applied out-of-plane magnetic field (top panels). The bottom panels show the Zeeman splitting ($\Delta = E_{\sigma^+} - E_{\sigma^-}$) from the corresponding IXs as a function of the applied magnetic field with a linear regression from which the values of the effective Landé g_{eff} of -15.89 and 6.72 are extracted. (C) Leftmost panel: PL spectrum showing a few moiré-trapped IXs in MoSe₂/WSe₂. The blue and red regions shown for the PL line at 1.401 eV represent the estimated PL signal from the emitter and the background, respectively. Second panel from the left: integrated PL intensity of the emitter highlighted in the leftmost panel at different excitation powers. Second panel from the right: second-order photon correlation statistics of the emitter highlighted in the leftmost panel. The red shadowed area represents the Poissonian interval error associated to the experimental determination of $g^{(2)}(\tau)$. The black dashed line and the gray shadowed area represent the average and error interval of the experimental limitation for $g^{(2)}(0)$, respectively, owing to the non-filtered emission background. Rightmost panel: PL spectra of moiré-trapped IXs in a dual-gated MoSe₂/WSe₂ hetero-bilayer at different gate voltages. Three representative peaks are indicated as E1, E2, and E3.

WSe₂/MoSe₂ hetero-bilayers also enables the formation of moiré-trapped interlayer triions, which are bound quasiparticles consisting of two electrons and a hole (negatively charged triion) or a single electron and two holes (positively charged triion) [66–69]. Upon electron or hole doping of the hetero-bilayer, the neutral trapped IXs form on-site negatively or positively charged interlayer triions with an average binding energy of ~ 7 and ~ 6 meV, respectively (see Figure 3A) [66–69]. Interestingly, the doping-dependent evolution of the IX PL shows the same overall behavior for both low and high IX densities (Fig-

ure 3B) [67, 69], with the only differences being: i) the emission line widths, which are one order of magnitude broader for the ensemble exciton peaks; and ii) the absolute emission energies, which show an exciton-density-dependent blue-shift in the ensemble exciton peaks as a consequence of the dipolar interactions [69]. Moreover, the magneto-optical properties of the neutral and charged IXs are also identical (see Figure 3C). However, at high IX densities, emission from a higher energy IX ensemble peak with opposite selection rules and different effective g-factor appears, which has been attributed to

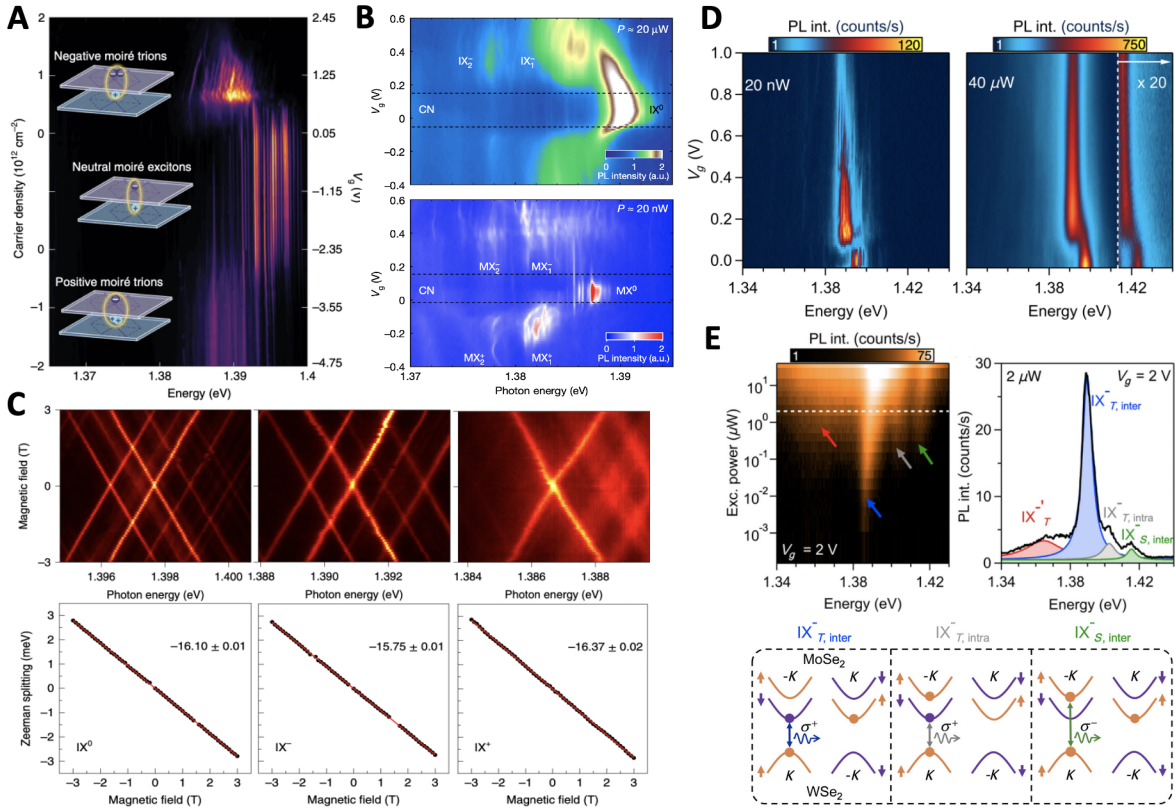


FIG. 3. Moiré-trapped interlayer triions in TMD hetero-bilayers [WSe₂/MoSe₂ (A-E)].

(A) Gate-dependent PL emission from a WSe₂/MoSe₂ hetero-bilayer showing PL from moiré-trapped interlayer excitons and triions. The positive (negative) gate voltage (V_g) and carrier density correspond to the electron (hole) doping. (B) Gate-dependent PL intensity of moiré-trapped IXs in a WSe₂/MoSe₂ hetero-bilayer for excitation powers of 20 μ W (top) and 20 nW (bottom). (C) Top: PL spectra of moiré-trapped neutral (left), negatively-charged (middle), and positively-charged (right) IXs as a function of a vertical magnetic field. Bottom: Zeeman splitting of representative IXs extracted from the corresponding top panels. Landé g_{eff} of -16.10, -15.75 and -16.37 are extracted for neutral IX⁰, negatively charged IX⁻ and positively charged IX⁺, respectively. (D) Gate-voltage-controlled PL of IXs in the neutral ($V_g \leq 0.1$ V) and electron-doping regime ($V_g \geq 0.1$ V) for excitation powers of 20 nW (left panel) and 40 μ W (right panel) at 4 K. In the right panel, the PL intensity is multiplied by a factor 20 in the spectral range delimited by the vertical dashed area for visualization purposes. (E) Right: Logarithmic-scale density plot showing the evolution of the PL spectrum of negative interlayer triions as a function of excitation power, in which four different peaks can be resolved (as indicated by the arrows). Left: PL spectrum acquired for an intermediate excitation power of 2 μ W (as indicated by the white dashed line in the left panel) showing four Lorentzian peaks corresponding to various exciton species. Bottom: Schematic representation of the charge configurations for IX⁻_{T,inter} (left), IX⁻_{T,intra} (middle), and IX⁻_{S,inter} (right) showing the optical transitions that involve a hole in the topmost valence band of WSe₂ at K. Adapted with permission from Ref. [66] (A), Ref. [67] (B), Ref. [68] (C), Nature Publishing Group, and Ref. [69] (D, E), American Physical Society.

optical transitions involving the highest spin-orbit-split conduction band of MoSe₂ at $\pm K$ [4, 69–71]. This higher energy ensemble exciton state can also be tuned from a neutral to a charged regime by gate doping, with a charging offset very similar to the ground IX state at lower energy (see Figure 3D)[69].

Finally, a combination of power-dependent and magneto-optical measurements in a gate-tunable MoSe₂/WSe₂ hetero-bilayer revealed the presence of three different species of moiré-localized negative triions with contrasting spin-valley configurations: intervalley interlayer triions with spin-singlet optical transitions, and

both intervalley and intravalley interlayer triions with spin-triplet optical transitions (as schematically depicted in the right, central, and left panels of the bottom of Figure 3E, respectively [69]), which result in PL spectra that can show up to four different PL components: the three moiré-localized negative triions with contrasting spin-valley configurations plus an additional low-energy peak which has recently been attributed to a composite six-particle “hexciton” state [72].

The presence of a long-range periodic exciton potential can profoundly modify the optical spectrum of TMDs. This is the case for twisted TMD homo- and hetero-bilayers, in which the moiré superlattice gives rise to a long-range crystal structure with a reduced Brillouin zone. The reduced Brillouin zone results in a folding-induced flattening of the conduction and valence bands and a multitude of avoided crossings that arise as a consequence of the interlayer hybridization [74, 77]. Recently, several groups have experimentally shown that the periodic moiré exciton potential leads to a mixing of momentum states separated by moiré reciprocal lattice vectors, which results in the formation of satellite exciton peaks (see Figure 4A) [73, 74]. Although the moiré superlattice plays a key role in the formation of the satellite peaks observed in these works (also referred to as Umklapp [73] or moiré excitons [74]), the origin of the periodic exciton potential is different. In Ref. [73], the authors used a twisted MoSe₂/hBN/MoSe₂ homo-bilayer structure where the carrier density in the two MoSe₂ layers can be controlled independently. The presence of the monolayer-thick hBN barrier layer in their device reduces the interlayer coupling between the twisted MoSe₂ layers, which results in a weak periodic moiré potential for intralayer excitons. Therefore, in the absence of electron or hole doping, the spectrum does not show any moiré exciton peaks (see Figure 4B). However, for unity electron filling of the underlying moiré potential in either or both MoSe₂ layers, new optical resonances appear in the reflection spectrum (see Figure 4B). Such Umklapp or moiré exciton resonances arise due to the spatially modulated interactions between excitons and electrons in an incompressible Mott-like correlated state, which creates a periodic potential for excitons with the periodicity imposed by the moiré lattice constant [73]. In contrast to the MoSe₂/hBN/MoSe₂ device in Ref. [73], nearly-aligned WSe₂/WS₂ hetero-bilayers present a strong static moiré potential, which leads to the formation of satellite moiré exciton peaks even in the absence of electron or hole doping (see Figure 4C) [74]. The presence of such satellite moiré exciton peaks is not restricted to hetero-structures consisting of two layers, but has also been reported in devices in which the WSe₂ layer is replaced by a bilayer and a trilayer [78].

Moreover, the moiré pattern of TMD hetero-bilayers has shown to result in the formation of non-trivial many-body excitonic states [79, 80]. Examples of such many-body moiré excitons include intralayer charge-transfer excitons [79] and an interlayer moiré exciton in which the hole's wavefunction is surrounded by the corresponding electron's wavefunction, which is distributed among three adjacent moiré traps [80].

In addition to the satellite spectral features caused by

Umklapp scattering within the reduced Brillouin zone and the presence on exotic many-body moiré excitons, the moiré effects on the intralayer excitons in TMD hetero-bilayers that feature a close energy alignment of the band edges (such as MoSe₂/WS₂ and MoTe₂/MoSe₂) are enhanced by resonant interlayer band hybridization [75]. Theoretical calculations show that the resonantly hybridized exciton energy in these TMD hetero-bilayers shows a sharp modulation as a function of the interlayer twist angle (see Figure 4D) [75]. Such resonant hybridization between exciton bands has been experimentally observed through PL measurements in WS₂/MoSe₂ [76], MoS₂/WSe₂ [84] and WS₂/WSe₂ [85] hetero-bilayers, which feature nearly-degenerate band edges. The hybridized excitons in these systems exhibit a pronounced energy shift as a function of twist angle (see Figure 4E) [76].

Hybridization of intralayer and interlayer exciton states

Intralayer and interlayer excitons in multi-layer TMDs can hybridize even in the absence of a moiré superlattice. The large quantum-confined Stark effect of IXs in TMD homo- and hetero-bilayers allows one to exploit the application of vertical electric fields to energetically tune IXs into resonance with intralayer excitons, where they hybridize [5, 37–39, 43, 44, 81, 82, 86, 87]. In the case homo-bilayer MoS₂, the results in Ref. [37] show that the Stark-split IX branches undergo clear avoided crossings with both the intralayer B- and A-exciton branches, where the coupling originates from hole tunnelling and from an exchange-induced A-B exciton admixture, respectively [86]. Similar couplings between interlayer and intralayer excitons have also been reported by other groups in bilayer 2H-MoS₂ [38, 39], natural bilayer and trilayer 2H-MoSe₂ [43], and three-, four-, five-, and seven-layer natural 2H-WSe₂ [44]. Figure 5A shows a density plot of the electric field dependence of the reflectance spectrum differentiated with respect to photon energy from trilayer 2H-WSe₂, where the hybridization of the IXs with the 1s and 2s states of the intralayer A exciton leads to clear anticrossings at the corresponding intralayer exciton energies [44].

In addition to the normalization of the exciton resonance energy and the redistribution of oscillator strength between the different exciton branches, the hybridization of interlayer and intralayer excitons in natural multi-layer 2H-stacked TMDs has also shown to result in gate-tunable g factors for the resulting hybrid exciton species [38, 43]. Figure 5B shows the electric-field-driven evolution of the g -factor of the hybrid excitons in a natural 2H-MoSe₂ bilayer [43] (bottom panel). The top panel shows the electric-field-dependent normalized contributions of each bare exciton state $|C^{IX(X)}|^2$ to the corre-

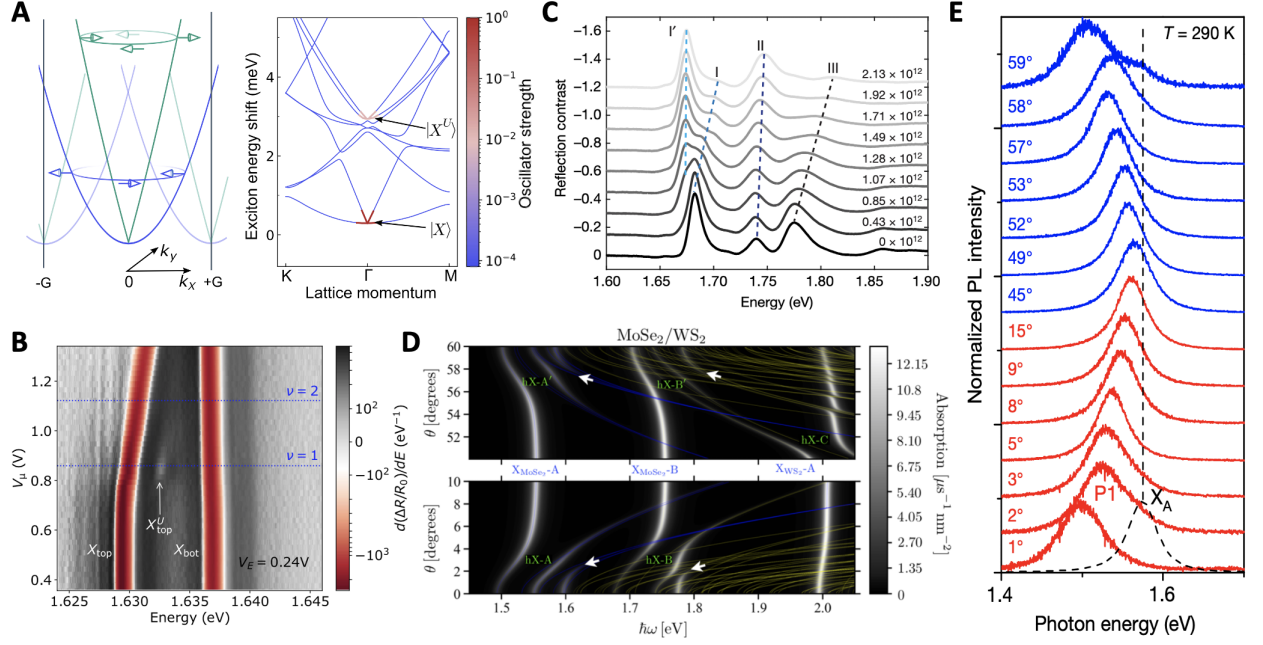


FIG. 4. Effects of the moiré superlattice on the intralayer excitons [MoSe₂/hBN/MoSe₂ (B), WS₂/WSe₂ (C), MoSe₂/WS₂ (D,E)].

(A) Left: bare dispersion of mobile excitons in a ML TMD. The linearly polarized exciton modes split into two branches with linear (green line) and parabolic (blue line) dispersion due to the strong intervalley electron-hole exchange coupling. The transparent lines represent higher bands arising from the mixing of states connected by reciprocal lattice vectors as a consequence of a periodic potential. Right: dispersion bands of excitons moving in periodic moiré potential along a path in the moiré Brillouin zone. The color bar indicates the oscillator strength of each state (saturated for all blue lines). Only a single Umklapp band per polarization obtains sizable oscillator strength, while most states remain dark. (B) Dependence of the differential reflectance measured in MoSe₂/hBN/MoSe₂ hetero-structure as function of the chemical potential V_μ differentiated with respect to energy E for a fixed vertical electric field $V_E = 0.24$ V. An additional higher-energy Umklapp exciton resonance X_{top}^U is observed once the top layer is filled with one electron per moiré site (i.e., $\nu = 1$). (C) Reflection contrast spectrum measured in a moiré WS₂/WSe₂ hetero-bilayer as a function of electron concentration. Three prominent moiré exciton peaks are labelled. Peak I exhibits a strong blue-shift and diminishes upon doping while another lower energy peak (I') emerges. Similarly peak III shows a strong blue-shift and weakens upon doping. (D) Calculated absorption spectrum as functions of twist angle for MoSe₂/WS₂ close to parallel (bottom panel) and anti-parallel (top panel) alignment. The full low-energy exciton spectrum is overlaid on top the absorption map by blue and yellow curves, showing multiple momentum-dark exciton states. (E) Normalized room-temperature PL spectra of MoSe₂/WS₂ hetero-bilayers with interlayer twist angles ranging from 1° to 59°. The dashed curve shows the typical room-temperature PL peak from the A exciton of ML MoSe₂ (X_A), and its energy is indicated by the vertical dashed line. Adapted with permission from Ref. [73] (A, B), Ref. [74] (C), Ref. [75] (D), Ref. [76] (E).

sponding hybrid excitons, showing a clear evolution from pure intralayer (interlayer) to pure interlayer (intralayer) character before and after the anticrossing.

The V_g -induced hybridization between intralayer and interlayer excitons is not restricted to natural TMD multilayers, but can also be observed in twisted TMD homo- and hetero-bilayers [5, 81, 82]. In Ref. [81], the coupling between intralayer and interlayer excitons in near-0°-twist-angle MoSe₂/MoSe₂ homo-bilayers is reported. These homo-bilayers featured large rhombohedral AB/BA domains, which support IXs with out-of-plane electric dipole moments in opposite directions that can be flipped by the application of vertical electric fields, resulting in field-asymmetric hybridization with

intralayer excitons (see Figure 5C). In Ref. [82], hybridization of interlayer and moiré excitons in angle-aligned WSe₂/WS₂ and MoSe₂/WS₂ hetero-bilayers was observed and in Ref. [87] for MoSe₂/WS₂ hetero-bilayer. The hybrid excitons are formed via spin-conserving resonant tunnelling of electrons or holes between the layers, and exhibit the characteristics of both interlayer (large out-of-plane electric dipole) and intralayer excitons (appreciable oscillator strength). Figure 5D shows the electric-field dependence of hybrid excitons in a WSe₂/WS₂ moiré superlattice loaded with one electron per site [82], where the energy-level anticrossing between the intralayer moiré excitons (higher energy peaks) and the IXs (lower energy peak) can be observed. Simi-

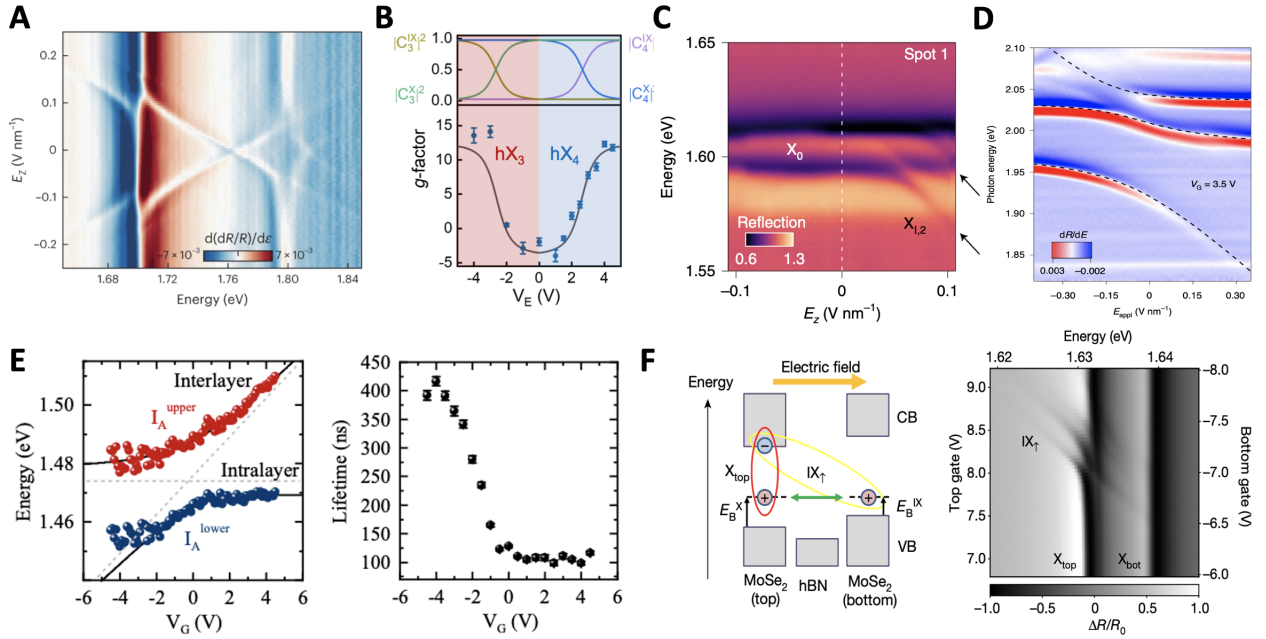


FIG. 5. Hybridization of intralayer and interlayer excitons [3L 2H-WSe₂ (A), 2L 2H-MoSe₂ (B), twisted ($t \approx 0^\circ$) MoSe₂/MoSe₂ (C), twisted ($t \approx 60^\circ$) WSe₂/WS₂ (D), MoS₂/WS₂ (E), MoSe₂/hBN/MoSe₂ (F)].

(A) Color maps of the reflectance spectrum differentiated with respect to photon energy from trilayer 2H-WSe₂ as a function of the electric field E_z applied perpendicular to the trilayer in the spectral regions around the ground and first-excited state of the A-exciton. (B) Electric-field-driven evolution of the g-factor of the hybrid inter- and intralayer excitons hX_3 and hX_4 in a natural 2H-MoSe₂ bilayer (bottom panel). The top panel shows the electric-field-dependent normalized contributions of each bare exciton state $|C^{IX(X)}|^2$ to the corresponding hybrid excitons. (C) Electric-field-dependent reflectance contrast spectra of the intralayer excitons in a near- 0° -twist-angle MoSe₂/MoSe₂ bilayer which features large rhombohedral AB/BA domains. (D) Energy derivative of the reflectance contrast spectrum as a function of the applied out-of-plane electric field in a 60° aligned WSe₂/WS₂ sample at a fixed doping of one electron per moiré cell. (E) Left panel: Emission energy of the upper (I_A^{upper}) and lower exciton branches (I_A^{lower}) in a MoS₂/WS₂ hetero-bilayer embedded in an vdW field-effect structure as a function of the applied gate voltage. Right panel: Hybridization-induced evolution of the PL lifetime corresponding to the lower exciton branch measured at a bath temperature of 10 K. (F) Color map of the reflectance signal from a MoSe₂/hBN/MoSe₂ as a function of the applied vertical electric field (right panel) together with the corresponding schematics of the energy bands and the exciton energy alignment (left panel). Adapted with permission from Ref. [44] (A), Ref. [43] (B), American Physical Society, Ref. [81] (C), Ref. [82] (D), Ref. [5] (E), and Ref. [83] (F), Nature Publishing Group.

lar electric-field-induced hybridization between interlayer and intralayer excitons was observed in angle-aligned MoS₂/WS₂ hetero-bilayers embedded in a vdW field-effect structure (see Figure 5E) [5]. In addition to the electric-field-induced energy anti-crossing between the upper and lower exciton branches in the PL spectra, the authors in Ref. [5] also showed hybridization-induced renormalization of the PL lifetime for the lower exciton emission branch (see Figure 5E). The electric-field-induced renormalization of the hybrid exciton resonance energies in all these systems can be quantitatively reproduced by a phenomenological model in which the hybridization between different exciton states is treated as a coupling between oscillators with resonance energies corresponding to the bare exciton states being hybridized [5, 38, 82]. The black dashed lines in Figures 5D and 5E show the best fits of the experimental data to an oscillator model, from which inter-/intralayer couplings as high

as 40 meV and 11 meV could be extracted, respectively, demonstrating that these systems were strongly coupled [5, 82].

Finally, the coupling between interlayer and intralayer excitons has been observed even for hetero-structures in which the interlayer exciton constituent states are located in layers separated by a hBN tunnel barrier [83]. Using a double-gated MoSe₂/hBN/MoSe₂ hetero-structure, coherent coupling of interlayer and intralayer excitons via hole tunnelling through the hBN barrier has been explored. Figure 5F shows a color map of the reflectance signal from the MoSe₂/hBN/MoSe₂ as a function of the applied vertical electric field, where the resonances at 1.632 eV and 1.640 eV correspond to intralayer excitons in the top and bottom MoSe₂ layers, respectively [83]. At large applied electric fields, several resonances with a strong E-field dependence are observed, which originate from IXs with a large dipole moment leading to a sizeable

Stark shift. The spectra for a positive top gate voltage (V_{tg}) regime correspond to the IX_{\uparrow} , which have a hole in the bottom layer and an electron in the top layer (see the schematic of the energy bands and the exciton energy alignment under electric fields in Figure 5F). Interestingly, the results in Figure 5F show that IX_{\uparrow} hybridize exclusively with intralayer excitons in the top layer, as seen by a multitude of avoided crossings, which unequivocally shows that the coupling originates exclusively from spin-conserving hole tunnelling. Finally, the existence of multiple avoided crossings demonstrates the existence of a moiré superlattice in the $MoSe_2/hBN/MoSe_2$ hetero-structure.

Structural effects on the PL of interlayer excitons

Beyond the effects of applied external electric fields, carrier doping, layer- and exciton-hybridization, and the moiré superlattice discussed in the previous sections, the structural properties of the TMD hetero-structures such as strain and atomic reconstruction also play an important role on the optical and electric properties of their host IXs. Recently, it has been shown that the PL of IXs in TMD homo- and hetero-bilayers can be profoundly affected by the structural properties of the hetero-structure [81, 88–90]. In Ref. [88], the authors used real-space imaging to show how the application of uniaxial hetero-strain in a $WSe_2/MoSe_2$ moiré hetero-bilayer, where the weak vdW interaction between the layers can result in different deformation, leads to a transition from a triangular moiré lattice of zero-dimensional traps into parallel stripes of one-dimensional quantum wires. Figure 6A illustrates the concept and shows experimental results for a nominally unstrained (top panels) and a strained hetero-bilayer (bottom panel). Interestingly, optical spectroscopy characterization of the samples revealed that the IX PL changes drastically from the unstrained to the strained samples. Figure 6B shows representative low-temperature PL spectra measured in nominally unstrained (top) and strained hetero-bilayers (bottom) for helicity-resolved photon collection. As can be seen in these plots, the PL emission from IXs in strained samples (i.e., depicting one-dimensional moiré potentials) shows linear polarization and two orders of magnitude higher intensity than the circularly-polarized quantum emitter-like sharp PL peaks characteristic of the zero-dimensional moiré traps.

In addition to active approaches to modify the IX emission through structural modifications of the TMD hetero-structures, intrinsic structural effects such as atomic reconstruction and domain formation in twisted hetero-structures [91–96] can also strongly alter the IX properties. In Ref. [81], a combination of electronic and optical far-field spectroscopy is employed to study near- 0° -twist-angle $MoSe_2/MoSe_2$ homo-bilayers featuring large

rhombohedral AB/BA domains (see the sketch in the top panel of Figure 6C). The bottom panel of Figure 6C shows a dark-field TEM image of one of their near- 0° -twist-angle $MoSe_2/MoSe_2$ homo-bilayers, where alternating, micrometre-sized AB and BA domains can be observed due to the effects of atomic reconstruction. Further, the authors showed that the broken mirror/inversion symmetry exhibited by the alternating AB/BA domains results into an effective locking of the domain atomic stacking and the orientation of the IX permanent dipole moment: AB (BA) domains host IXs with permanent electric dipole pointing up (down) [81]. This effect leads to opposite energy Stark shifts for IXs in AB and BA domains under applied vertical electric fields. Figure 6D shows electric-field-dependent PL spectra of IXs measured at three different spots in a twisted $MoSe_2/MoSe_2$ homo-bilayer (first three panels from the left) [81]. As can be seen in the first two panels, the IXs in two of the measured spots show field-dependent Stark shifts with similar magnitude but opposite signs, indicating that the excitons in the two spots presented opposite dipole moments (as schematically shown in the insets). Interestingly, these measurements also showed that the dipole orientation in both spots can be flipped at large enough applied fields. The results of a third spot demonstrate IX with Stark shifts with both positive (blue-shift) and negative (red-shift) slopes, indicating the presence of both AB and BA domains inside the dimensions of the confocal PL spot. The authors were also able to exploit the domain-dependent sign of the IX Stark shift to generate a spatial map of the electric dipole moment of the IX in their sample (see right panel in Figure 6D).

Finally, in Ref. [96] the authors showed one-to-one correlations between local spectral features and sample morphology in non-gated $MoSe_2/WSe_2$ hetero-bilayers, which suggests the co-existence of domains of different dimensionality and exciton characteristics. Their results show that reconstructed 2D domains with large lateral dimensions in small-twist hetero-bilayers exhibit clear luminescent singlet and triplet IXs while split intralayer exciton resonances and spectrally narrow IXs are present in the 1D domains connecting the extended 2D domains to arrays of nanometre-sized 0D domains.

INTERACTIONS

Interlayer excitons interacting with electronic states in moiré hetero-structures

First predicted theoretically in 2018 [99, 100], it has been experimentally shown that strong electronic correlations can arise in the flat-bands of TMD hetero-structures that arise due to the moiré superlattice structure [18, 19, 83, 101]. In this scenario, the flat bands quench the kinetic energy of the charge carriers relative

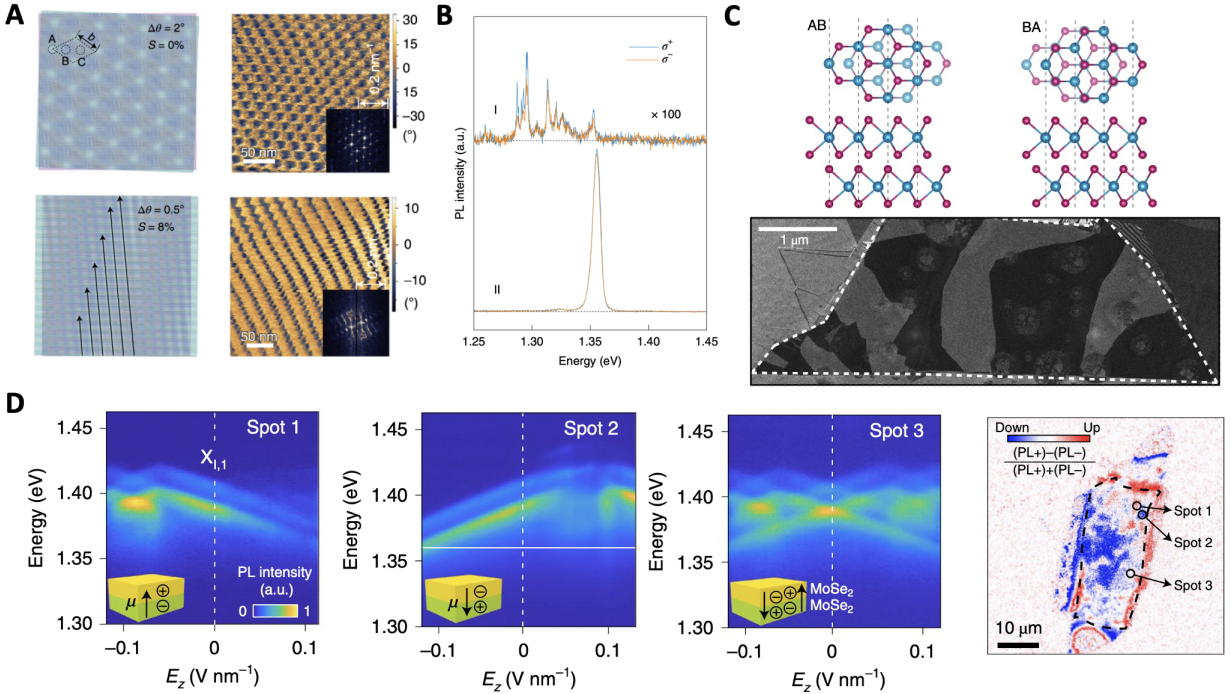


FIG. 6. Structural effects on the PL of interlayer excitons [MoSe₂/WSe₂ (A, B) and twisted MoSe₂/MoSe₂ (C, D)].

(A) Top left: sketch of a MoSe₂/WSe₂ hetero-bilayer with a twist angle of 2° at no applied strain. The dashed lines indicate the supercell of the hexagonal moiré superlattice, where A, B and C represent high-symmetry points preserving the C₃ symmetry within the supercell. Bottom left: sketch of a MoSe₂/WSe₂ hetero-bilayer with a twist angle of 0.5° under an applied uniaxial hetero-strain of 8%. The arrows indicate the resulting primary 1D moiré structures. Right panels: experimental piezoresponse force microscopy (PFM) images of the same spatial spot in a MoSe₂/WSe₂ hetero-bilayer with a twist angle of ~59° under no applied (top) and applied uniaxial strain (bottom). (B) Representative PL spectra from two MoSe₂/WSe₂ hetero-bilayer samples with h-BN encapsulation showing circularly-polarized quantum emitter-like sharp PL peaks (top) and linearly-polarized ensemble IX emission (bottom). The blue and orange lines represent helicity-resolved spectra for σ^+ and σ^- emission, respectively, under σ^+ excitation. (C) Top panels: top and side views of the atomic structure in a twisted MoSe₂/MoSe₂ homo-bilayer showing rhombohedral AB (left) and BA stacking configurations (right). Bottom panel: dark-field TEM image of a near-0°-twist-angle MoSe₂/MoSe₂ bilayer showing alternating, micrometre-sized AB and BA domains. (D) Electric-field-dependent PL spectra of IXs measured at three different spots of a twisted MoSe₂/MoSe₂ homo-bilayer (first three panels from the left). The insets show sketches of the predominant orientation of the permanent electric dipole at each spot. The right panel shows a map of the magnitude $(PL^+ - PL^-)/(PL^+ + PL^-)$, which is proportional to the orientation (up/down) of the permanent electric dipole. PL^\pm is the PL intensity at $E_z = \pm 0.15 \text{ V nm}^{-1}$, integrated over the energy range below 1.36 eV. Adapted with permission from Ref. [88] (A, B), and Ref. [81] (C, D), Nature Publishing Group.

to their Coulomb interaction energy, and several stable charge ordered phases, designated as Wigner crystals and Mott insulators, are observed at multiple fractional fillings (ν) of the moiré lattice. Selected examples of ordered states are shown in Figure 7A.

Initially, the charge ordered states were optically probed using the dielectric response of IXs to the correlated electronic states [18, 19, 83, 101]. However, due to their large permanent dipole, IXs are not only highly tunable with applied electric field, but they are highly sensitive to their charge environment. Natural questions to ask then, is how do the correlated electronic phases affect the IX emission and can one use the trapped IX as a sensitive local probe of the electronic crystallization in the vicinity of the IX? In addition to use IXs as local

probes, novel many-body ground states are formed via the interaction of moiré excitons and correlated electron lattices.

In a WSe₂/WS₂ moiré hetero-structure, Liu et al. investigated the PL from IXs as a function of fractional filling of the moiré lattice [21]. Abrupt changes in PL intensity and photon energy are observed at a number of different fractional fillings corresponding to correlated insulating states at $\nu = -2, -3/2, -8/7, -1, -1/3, -1/4, 1/4, 1/3, 2/5, 2/3, 6/7, 1, 5/4, 5/3, \text{ and } 13/7$. This modulation can arise because the insulating phases have reduced charge screening which renormalizes the band gap and exciton (or trion) binding energy. Further, the valley polarization is modulated by the charge ordered states. The degree of valley polarization is measured by

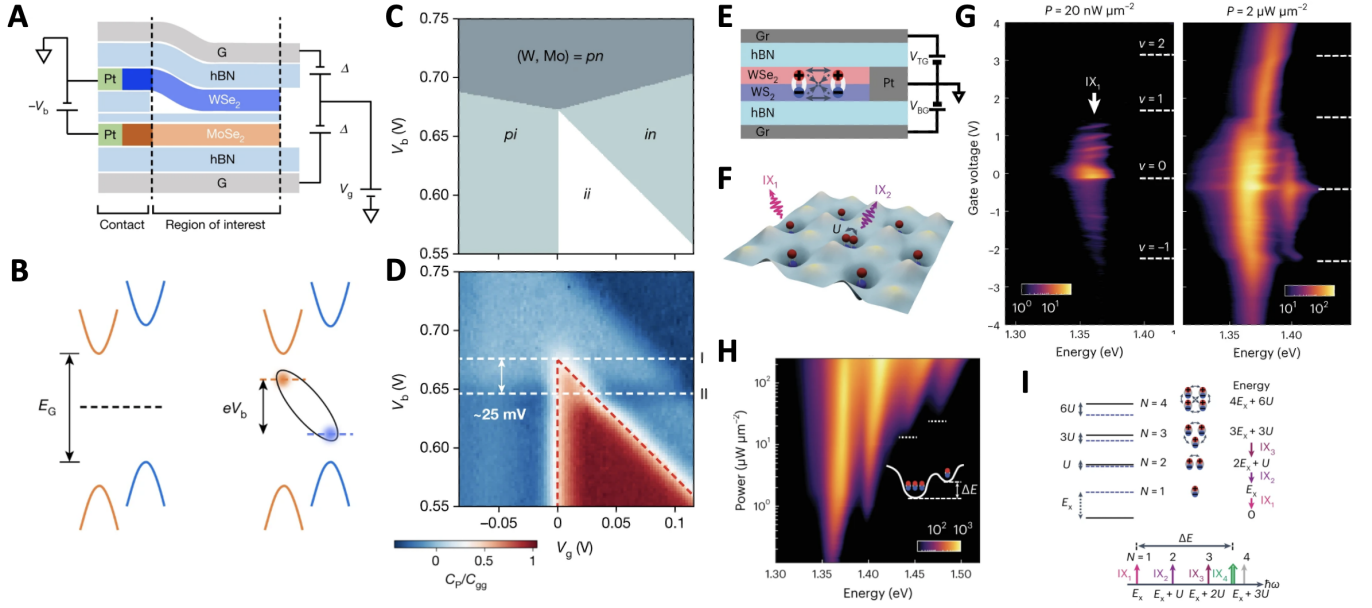


FIG. 7. Excitonic insulators in moiré superlattice structures [WSe₂/hBN/MoSe₂ (A-D), WSe₂/WS₂ (E-I)]. (A) Schematic of dual-gated bilayer devices. Anti-symmetric gating Δ reduces the gap energy E_G . The symmetric gating V_g tunes the electron and hole density difference. (B) Scheme of the type II band alignment of MoSe₂/WSe₂. A bias voltage V_b reduces the charge gap. IXs can form. (C) Electrostatics simulation of the bilayer based on a parallel-plate capacitor model. Depending on bias and gate voltages, the bilayer can be in an intrinsic (i), positively (p) and negatively (n) doped regime. (D) Normalized penetration capacitance C_P/C_{gg} as a function of bias and gate voltages (C_{gg} gate-to-gate capacitance). Charge incompressible region is marked by red dashed lines. The estimated exciton binding energy in the limit of zero exciton density is 25 meV. (measurements done at 15 K and $\Delta = 4.6$ V). (E) Schematic of a dual-gated WSe₂/WS₂ hetero-bilayer. (F) Illustration of the moiré exciton lattice with one of the moiré unit cells with double occupancy. (G) IX PL intensity as a function of gate voltage (doping) and emission energy for low (left) and high optical excitation intensity (right). Filling factors are labelled. With increasing excitation intensity, the PL peak IX_2 (34 meV above the ground state) appears. (H) IX PL intensity versus excitation power P . The threshold P_{th} for the occurrence of IX_3 and IX_4 is marked by dashed lines. (I) Energy level diagram for a single moiré orbit occupied by multiple exciton dipoles. Solid (dashed) line indicates the scenario with (without) onsite dipole-dipole interaction. Expected PL spectrum from the dipole ladder with constant energy spacing between IX_1 and IX_3 . IX_4 originates from the fourth exciton localized in the second moiré orbital and has hence lower energy. Adapted with permission from Ref. [97] (A-D) and from Ref. [98] (E-I).

spectrally integrating the PL intensity ratio $(I_{RR} - I_{RL}) / (I_{RR} + I_{RL})$, where the subscripts RR and RL indicate excitation-detection right- and left-handed circular polarization. The degree of valley polarization clearly decreases at the transition from conducting to insulating states. The valley polarization is limited by intervalley scattering and thus dependent on the electron-hole exchange interaction, which increases when the screening effect is reduced. Hence, in the insulating states, the intervalley scattering is increased and the valley polarization reduced.

Excitonic insulators in moiré structures

IXs with at least one constituent residing in a moiré-flat band are prone to form correlated bosonic states similar to the fermionic Mott-insulator state. Experimental observations of excitonic insulator states in TMD

hetero-structures are reported for various material combinations [24, 98] including natural bilayers [22, 23] and with ultrathin hBN separation layer [97] as shown in Figure 7(A). Strong onsite dipole-dipole interaction of excitons occupying the same moiré lattice is reported for WSe₂/WS₂ bilayers with the interaction between those IXs given by the Hubbard U parameter [98] (see Figure 7 (E, F)). PL measurements reveal a dipole ladder with emission peak separation of around 34 meV as summarized in Figures 7 (G-I). The authors conclude from such a large Hubbard parameter that in such systems exciton crystal phases can be possibly realized [98]. Signatures for the formation of an incompressible IX state in a MoS₂/hBN/WSe₂ hetero-structure has been deduced from capacitance measurements in Ref. [97] (see Figures 7 (C-D)). An incompressible state in this context means that the chemical potential of the system increases discontinuously as a function of exciton density [102]. Similarly, signatures for the formation of an incompress-

ible exciton state formed in $\text{WS}_2/\text{bilayer WSe}_2$ hetero-junction moiré superlattice for exciton filling factor $\nu=1$ have been observed by utilizing microwave impedance microscopy and differential reflectance spectroscopy $\Delta R/R$ [22]. Those signatures exhibit a peculiar temperature dependence and vanish above a critical temperature of about 90 K, suggesting the formation of an exciton insulator state of IXs at low temperatures [22]. Interestingly, Xiong et al. report the phase diagram for a mixed fermionic and bosonic correlated insulator for 60° -aligned WSe_2/WS_2 [24]. The excess electron density n_{ex} and the exciton density n_X were experimentally controlled and the mixed correlated insulator state has been observed along the line of $n_{tot} = n_{ex} + ne = 1$. Again, the exciton correlated insulator states are experimentally identified by their incompressible nature determined by a special type of optical pump-probe spectroscopy in analogy to the electrical capacitance measurements [24].

Degenerate ensembles of mobile interlayer excitons

At low temperatures and high exciton densities, thermalized ensembles of mobile IXs can be considered to be degenerate in vdW hetero-bilayers, as soon as the excitonic thermal de-Broglie wavelength exceeds the mutual distance between the IXs [103, 104]. The corresponding phase diagram includes this degeneracy phase with a predicted local superfluidity at a temperature below 10s of Kelvin and a possible Berezinskii–Kosterlitz–Thouless transition to a phase with an expected macroscopic superfluidity at even lower temperatures [105]. At high exciton densities (above $\sim 10^{12} \text{ cm}^{-2}$), a Mott transition to a degenerate electron-hole Fermi gas is expected wherein fermionic interactions between the electrons and holes dominate [104, 105]. Recently, it was proposed that also for the degenerate phase both the fermionic and bosonic characteristics of the exciton ensembles need to be considered, particularly at the presence of phonons [106].

The coherence of the ground state of such many-body ensembles can be deduced from the temporal and spatial coherences as measured in luminescence experiments (see Figures 8A and [3, 107–115]). For such experiments, IXs are advantageous compared to intralayer excitons due to their relatively long lifetime of tens to hundreds of nanoseconds [1, 2, 116, 117] and a permanent dipole moment [5] (see above sections). The long lifetime allows performing time-resolved experiments, such that the IX ensembles can be considered to be thermalized before they emit a photon [107, 117], while the out-of-plane dipole drives an in-plane expansion of the IXs. In turn, the IX mobility can be straight-forwardly “imaged” as soon as the spatial luminescence pattern exceeds the optical excitation area (Figures 8B and section below, [118–128]). Recent experimental work on $\text{MoSe}_2/\text{WSe}_2$ hetero-bilayers suggests that IX ensembles particularly

with a Lorentzian luminescence profile allow accessing coherent phases of dense and mobile IXs, consistent with the predicted quantum degeneracy at low temperature [3, 107]. In contrast, Gaussian luminescence profiles with possible sub-structures appear at higher temperatures and/or at the presence of additional localized excitons (cf. Figures 8A and above sections).

In principle, luminescence experiments allow distinguishing whether bosonic or fermionic interactions dominate within the ensembles of mobile IXs: for an increasing exciton density, a decrease of the full-width at half maximum (FWHM) of homogeneously broadened luminescence spectra is understood as a signature for a dominating bosonic characteristic within the exciton ensembles [106]. A corresponding increase of the FWHM is less unambiguous, pointing towards fermionic interactions, but also towards the interaction with further particles, such as phonons [106, 129, 130]. The temporal coherence of the luminescence can be accessed by the help of Michelson-Morley interferometers. The corresponding coherent part of the interferometers’ signal is expressed as the normalized first order correlation function $|g^{(1)}(\tau)|$ [131], with τ the time delay between the two optical paths within the interferometer (cf. Figures 8C). Particularly, a bi-exponential decay of $|g^{(1)}(\tau)|$ as in Figures 8C allows accessing the homogeneously broadened (Lorentzian) part of a luminescence spectrum (cf. Figures 8A and [131]). Recent work suggests that degenerate ensembles of mobile IXs in $\text{MoSe}_2/\text{WSe}_2$ hetero-bilayers show such a coherent luminescence of “synchronized” emitters [3], with the temporal coherence time, the FWHM of $|g^{(1)}(\tau)|$ being in the regime of 100s of fs. At present, this fast time scale is related to the emission process of the photons. At higher temperatures, when the IX ensembles are expected to be in the phase of a non-degenerate, classical gas, the corresponding $|g^{(1)}(\tau)|$ is reduced and it seems to follow a Gaussian profile (cf. Figures 8C and [107]).

For measuring the spatial coherence of the IXs’ luminescence, it is essential that the spatial pattern of the excitonic luminescence is isotropic in the plane of the hetero-bilayer (e.g. Figures 8B) and that the point-spread function (PSF) of the utilized optical system both at the wavelength of the optical excitation and detection is thoroughly understood [107]. Then, with the help of a point-inverting Michelson-Morley interferometer [132, 133], the spatial dependence of the normalized first order correlation function $|g^{(1)}(x, y)|$ can be imaged, with x and y the coordinates within the reference frame of the hetero-bilayers (cf. Figures 8D). Importantly, such spatial coherence experiments need to be performed again in a time-resolved manner, because only when the excitation laser is off for several 100s of fs to ps, laser-induced coherences as well as thermalization dynamics within the hetero-bilayers can be excluded to impact the IXs’ luminescence [107]. The lat-

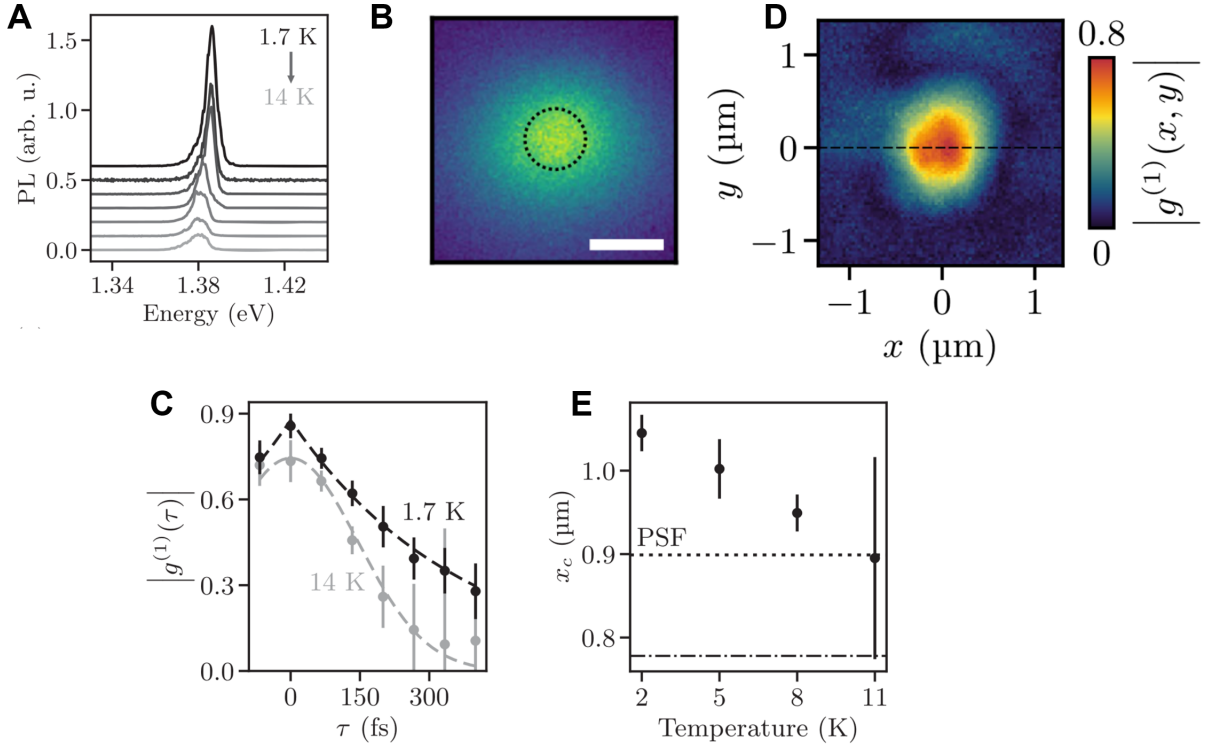


FIG. 8. Degenerate ensembles of mobile IXs and the coherence of their luminescence [MoSe₂/WSe₂ (A - E)]. (A) PL spectra from a MoSe₂/WSe₂ hetero-bilayer with h-BN encapsulation at the bath temperature ranging from 1.7 K to 14 K. The maximum at ~ 1.38 eV corresponds to IXs. (B) Corresponding spatial PL map in a false-color plot at 1.7 K [green (blue) equals high (low) intensity], demonstrating an isotropic expansion of the IXs in the plane of the hetero-bilayer. Dotted circle highlights the point spread function (PSF) at the IX wavelength (1.38 eV ~ 0.9 μm). Scale bar, 1 μm . (C) Normalized first order correlation function $|g^{(1)}(\tau)|$ of the IX luminescence for 1.7 K and 14 K, with τ the time delay as given by a Michelson-Morley interferometer. (D) Spatial dependence of the normalized first order correlation function $|g^{(1)}(x, y)|$ at $\tau = 0$. (E) Temperature dependence of the spatial coherence length x_c . Dotted and dashed-dotted lines represent the point spread function PSF at the emission wavelength [as in (B)] and the excitation energy (1.94 eV ~ 639 nm). Adapted with permission from Ref. [107]

eral FWHM of $|g^{(1)}(x, y)|$, e.g. as measured along the dashed line in Figure 8D, gives access to the spatial coherence length x_c of the IXs' luminescence. Recent experiments on MoSe₂/WSe₂ hetero-bilayers demonstrate that x_c can exceed the PSFs of the optical imaging apparatus at the experimental temperature when the IXs can be theoretically considered to be degenerate (cf. Figure 8E and [107]). Then, x_c can be even equal to the overall expansion of the IXs ensembles [107]. Future studies, e.g. on laterally patterned hetero-bilayers [121, 134–136], might reveal whether the predicted local or macroscopic superfluidity explains the extended spatial coherence of the luminescence. Moreover, for an unambiguous experimental evidence of a pure bosonic exciton condensation in the momentum space, back-focal plane imaging seems to be suitable, however, at temperatures significantly below 1K [137].

Dynamics of interlayer excitons: formation and transport

As discussed, in most TMD-based hetero-bilayer type-II band alignment with efficient IX formation upon separation of electron and hole states in adjacent layers is commonly reported. Already in 2014, Hong et al. [138] experimentally demonstrated ultrafast interlayer charge transfer withing 50 fs of photo-excited carriers across the vdW gap in MoS₂/WS₂ hetero-bilayers. This process is surprisingly fast since the photoexcited carriers are supposed to live at the *K*-valley formed by transition-metal *d*-orbitals that are well localized within each layer such that tunneling over the vdW gap is required for charge transfer [139]. Combined experimental and theoretical effort established that this ultrafast charge transfer is mediated by efficient intervalley phonon scattering connecting the layer localized CB *K*-states with the strongly hybridized Σ -states facilitating ultra-

fast charge transfer [139–143]. By femtosecond momentum microscopy together with microscopic modelling, the authors in Ref. [143] showed that momentum indirect $\Sigma - K$ intralayer excitons and layer hybridized $h\Sigma - K$ -IXs form via exciton-phonon scattering in WSe₂ monolayers and WSe₂/MoS₂ hetero-bilayers, respectively. Interestingly, the relative level alignment between the direct $K - K$ - and the indirect (h) $\Sigma - K$ -excitons matters in the radiative decay process. If the Σ -states are energetically lower compared to K as in the hetero-bilayer, an exciton cascade transfers the $K - K$ -exciton over the $h\Sigma - K$ into a true IX [143]. For a (nearly) degenerate alignment, as in WSe₂ monolayers, the exciton occupation decays predominantly radiatively via the bright $K - K$ -exciton indicating the crucial role of level alignment that is prone to changes by internal and external stimuli such as embedding in vdW stacks that can e.g. impact interlayer hybridization or interlayer phonon coupling, dielectric environment, doping or strain and is hence is highly tunable [143, 144]. The crucial role of the phonons in these ultrafast charge transfer processes has been directly confirmed from ultrafast electron diffraction visualizing the lattice dynamics in photoexcited WSe₂/WS₂ [145].

Several partially competing impact factors underlie the transport properties of excitons species in vdW bilayer structures resulting in a wealth of different scenarios [6, 146–148]. Moiré superlattice potential modulation can result in nearly complete localized excitons while shallow twist and/or high IX densities foster tunneling between moiré sites resulting in hopping transport such that the diffusion length is highly dependent on materials combination and twist angle and can even reach a few microns in commensurate vdW bilayers [148–151]. IXs with constituents localized in adjacent layers hold a permanent dipolar moment such that dipole-dipole interaction, i.e. repulsion modulates exciton transport in vdW bilayers and allows for long-range propagation [6, 147]. Large linear diffusion coefficients even at low IX densities have been shown for reconstructed, low-disorder MoSe₂/WSe₂ hetero-bilayers at cryogenic temperatures [147]. Non-linear propagation in those structures arise from nearly equally contribution from exciton-exciton repulsion and annihilation [147]. Layer hybridized IXs have a reduced out-of plane dipolar moment and dipolar interaction contributes less to exciton transport. Tagarelli et al. demonstrate that the degree of hybridization can be tuned by electric fields enabling control of IX transport in vdW hetero-bilayers [6]. Understanding and controlling of exciton transport in vdW bilayer structures is important for both the realization of efficient excitonic and optoelectronic devices.

CONCLUSION AND OUTLOOK

We introduced the fundamental concepts of how the interplay of spins, valley degree of freedom, moiré superlattice formation, doping as well as external stimuli determine the properties of exciton species in homo- and hetero-bilayer TMD devices. The interplay of the different degrees of freedom is dictated by the precise details of the stacking of the bilayer TMDs such that their properties can be widely engineered. This review provides a snapshot of the state-of-the-art experimental demonstrations in the field, including the first devices that provide technological implementations that exploit the novel properties of IXs in moiré materials. Altogether, these results establish a strong foundation for a wide range of future fundamental studies and developing technologies. In the following, we provide a perspective on future challenges and a few worthwhile pursuits in this rapidly emerging topic.

One exciting prospect is exploiting the highly tunable properties of trapped IXs as quantum light sources. Because of the IXs' large permanent dipole, DC Stark tuning of the exciton energy over a wide range is facile. So far, the quantum nature of the emission has been demonstrated with individual IXs trapped via the intrinsic moiré potential, but an additional avenue to pursue is extrinsic trapping of IXs for quantum light sources, for example via localized strain or electrostatic potential via tunable gating [152–154]. The externally generated potentials for trapping can enable deterministic positioning and scalability for applications in quantum photonics. For these applications, nanophotonic structures will be required to achieve Purcell enhancement and increased light-matter interaction efficiencies. An open question is how coherent the generated photons can be; can highly indistinguishable photons be generated in these platforms? Similarly, open questions exist about the potential to exploit the spin-valley degrees of freedom of trapped IXs to enable a coherent spin-photon interface. On the other hand, the intrinsically high density of precisely arranged quantum emitters in the moiré lattice provides a platform for investigations of sub- and super-radiant Dicke states with applications in quantum information science.

From a many-body physics point of view, the long lifetimes and strong dipolar interactions of Bosonic neutral IXs in TMD moiré materials can yield correlated excitonic states, as described by the Bose-Hubbard model. Changing the band structure (determined by the material combinations), moiré period and exciton density provide access to a wide range of the Bose-Hubbard phase diagram in different regimes such as non-interacting Bose gas phase, superfluid phase, quadrupolar and dipolar exciton ensembles, Mott insulator phase or beyond the Mott transition an electron-hole plasma phase [155–159].

By adding a charge to the localized, neutral excitons via electrostatic gating, charged Fermi-polarons can be created, providing access to the Fermi-Hubbard model. Overall, a significant goal in the field is to realize designer many-body Hamiltonians in moiré superlattices as a new platform for quantum simulators. Employing IXs as probes of these systems remains a compelling concept. Moreover, for MoSe₂/WSe₂ hetero-bilayers, reported signatures of degenerate exciton ensembles with an extended lateral coherence [3, 107] suggest that hetero-bilayers also allow studying bosonic and fermionic correlations in mobile exciton ensembles. In addition to tuning the phase diagram by the stacking configuration during fabrication, an important target will be to *in-situ* tune the interaction parameters. Two approaches can readily be pursued: applying hetero-strain to tune the geometry of the moiré lattice [160] or controlling the relative twist angle between the bilayers [161].

To date, most TMD moiré devices have consisted of only a handful of individual atomic layers; due to poor fabrication yield, a device consisting of a few TMD layers encapsulated in hBN layers and electronic gating with graphene layers is considered a ‘hero’ device in many laboratories. This limits the boundless opportunities to freely engineer and add to the many degrees of freedom for dipoles in multilayer devices. For instance, spin-layer locking adds an additional layer degree of freedom in the system while giant interlayer dipoles extending over more than two-layers can in principle be engineered. Further, multilayer devices with independently configurable hetero-interfaces yield exciting prospects such as multi-orbital moiré superlattices or multiple moiré periodicities of varying moiré potential strength.

A final challenge, not solely confined to moiré TMD devices but for the entire field of vdW moiré materials, is the development of improved fabrication techniques that take steps towards reproducible and homogeneous moiré superlattices with deterministic periodicity. Current state-of-the-art fabrication techniques yield significant inhomogeneities within the moiré superlattice, including twist angle disorder and defects such as bubbles or wrinkles. Additionally, substantial sample-to-sample variation presents reproducibility issues across different laboratories. Important questions to address include “How homogeneous can a moiré material be?” and “How does twist-angle disorder affect or determine the emergent physical properties of the moiré material?” Further, increased reproducibility and moiré homogeneity are essential to realize more complex samples and devices with increasing number of layers and contacts. Finally, improved and reproducible low-resistance Ohmic contacts to TMDs would facilitate transport measurements on a regular basis, a crucial technique which can compliment optical investigations of moiré TMD devices.

AUTHORS CONTRIBUTIONS

All authors discussed the content of the manuscript and wrote it together.

FUNDING

We gratefully acknowledge financial support from the German Science Foundation via Grants HO 3324/9-2, WU 637/4-2 and 7-1, the clusters of excellence MCQST (EXS-2111) and e-conversion (EXS2089), and the priority program 2244 (2DMP). M.B.-G. is supported by a Royal Society University Research Fellowship. B.D.G. is supported by a Chair in Emerging Technology from the Royal Academy of Engineering and the European Research Council (grant no. 725920)

COMPETING INTERESTS

There is no conflict of interest.

DATA AVAILABILITY

Included in cited original research papers.

* m.brotons_i_gisbert@hw.ac.uk

† B.D.Gerardot@hw.ac.uk

‡ holleitner@wsi.tum.de

§ wurstbauer@uni-muenster.de

- [1] Pasqual Rivera, John R. Schaibley, Aaron M. Jones, Jason S. Ross, Sanfeng Wu, Grant Aivazian, Philip Klement, Kyle Seyler, Genevieve Clark, Nirmal J. Ghimire, Jiaqiang Yan, D. G. Mandrus, Wang Yao, and Xiaodong Xu, “Observation of long-lived interlayer excitons in monolayer MoSe₂-WSe₂ heterostructures,” *Nature Communications* **6**, 6242 (2015), number: 1 Publisher: Nature Publishing Group.
- [2] Bastian Miller, Alexander Steinhoff, Borja Pano, Julian Klein, Frank Jahnke, Alexander Holleitner, and Ursula Wurstbauer, “Long-Lived Direct and Indirect Interlayer Excitons in van der Waals Heterostructures,” *Nano Letters* **17**, 5229–5237 (2017), publisher: American Chemical Society.
- [3] Lukas Sigl, Florian Sigger, Fabian Kronowetter, Jonas Kiemle, Julian Klein, Kenji Watanabe, Takashi Taniguchi, Jonathan J. Finley, Ursula Wurstbauer, and Alexander W. Holleitner, “Signatures of a degenerate many-body state of interlayer excitons in a van der Waals heterostack,” *Physical Review Research* **2**, 042044 (2020), publisher: American Physical Society.
- [4] Alberto Ciarrocchi, Dmitrii Unuchek, Ahmet Avsar, Kenji Watanabe, Takashi Taniguchi, and Andras Kis, “Polarization switching and electrical control of inter-

- layer excitons in two-dimensional van der Waals heterostructures,” *Nature Photonics* **13**, 131–136 (2019).
- [5] Jonas Kiemle, Florian Sigger, Michael Lorke, Bastian Miller, Kenji Watanabe, Takashi Taniguchi, Alexander Holleitner, and Ursula Wurstbauer, “Control of the orbital character of indirect excitons in MoS₂/WS₂ heterobilayers,” *Physical Review B* **101**, 121404 (2020).
 - [6] Fedele Tagarelli, Edoardo Lopriore, Daniel Erckensten, Raúl Perea-Causín, Samuel Brem, Joakim Hagel, Zhe Sun, Gabriele Pasquale, Kenji Watanabe, Takashi Taniguchi, Ermin Malic, and Andras Kis, “Electrical control of hybrid exciton transport in a van der waals heterostructure,” *Nature photonics* **17**, 615–621 (2023).
 - [7] Mauro Brotons-Gisbert, Alfredo Segura, Roberto Robles, Enric Canadell, Pablo Ordejón, and Juan F Sánchez-Royo, “Optical and electronic properties of 2H-MoS₂ under pressure: Revealing the spin-polarized nature of bulk electronic bands,” *Physical review materials* **2**, 054602 (2018).
 - [8] Paul Steeger, Jan-Hauke Graalmann, Robert Schmidt, Ilya Kuppenko, Carmen Sanchez-Valle, Philipp Marauhn, Thorsten Deilmann, Steffen Michaelis de Vasconcellos, Michael Rohlfing, and Rudolf Bratschitsch, “Pressure dependence of intra- and interlayer excitons in 2h-mos2 bilayers,” *Nano Letters* **23**, 8947–8952 (2023), pMID: 37734032, <https://doi.org/10.1021/acs.nanolett.3c02428>.
 - [9] Viviana Villafañe, Malte Kremser, Ruven Hübner, Marko M. Petrić, Nathan P. Wilson, Andreas V. Stier, Kai Müller, Matthias Florian, Alexander Steinhoff, and Jonathan J. Finley, “Twist-dependent intra- and interlayer excitons in moiré mose₂ homobilayers,” *Phys. Rev. Lett.* **130**, 026901 (2023).
 - [10] Nihit Saigal and Ursula Wurstbauer, “Excitons stabilize above the band gap in bilayer wse2,” *Nature Nanotechnology* **19**, 141–142 (2024).
 - [11] Ka Wai Lau, Calvin, Zhirui Gong, Hongyi Yu, and Wang Yao, “Interface excitons at lateral heterojunctions in monolayer semiconductors,” *Phys. Rev. B* **98**, 115427 (2018).
 - [12] Jun Kang, Jingbo Li, Shu-Shen Li, Jian-Bai Xia, and Lin-Wang Wang, “Electronic structural Moiré pattern effects on MoS₂/MoSe₂ 2D heterostructures,” *Nano Letters* **13**, 5485–5490 (2013).
 - [13] Fengcheng Wu, Timothy Lovorn, Emanuel Tutuc, and A. H. MacDonald, “Hubbard model physics in transition metal dichalcogenide moiré bands,” *Phys. Rev. Lett.* **121**, 026402 (2018).
 - [14] H Baek, M Brotons-Gisbert, ZX Koong, A Campbell, M Rambach, K Watanabe, T Taniguchi, and BD Gerardot, “Highly energy-tunable quantum light from moiré-trapped excitons,” *Science Advances* **6**, eaba8526 (2020).
 - [15] Isaac Soltero, Mikhail A. Kaliteevski, James G. McHugh, Vladimir Enaldiev, and Vladimir I. Fal’ko, “Competition of moiré network sites to form electronic quantum dots in reconstructed mox₂/wx₂ heterostructures,” *Nano Letters* **24**, 1996–2002 (2024), pMID: 38295286, <https://doi.org/10.1021/acs.nanolett.3c04427>.
 - [16] Xiaobo Lu, Petr Stepanov, Wei Yang, Ming Xie, Mohammed Ali Aamir, Ipsita Das, Carles Urgell, Kenji Watanabe, Takashi Taniguchi, Guangyu Zhang, Adrian Bachtold, Allan H. MacDonald, and Dmitri K. Efetov, “Superconductors, orbital magnets and correlated states in magic-angle bilayer graphene,” *Nature* **574**, 653–657 (2019).
 - [17] Yanhao Tang, Lizhong Li, Tingxin Li, Yang Xu, Song Liu, Katayun Barmak, Kenji Watanabe, Takashi Taniguchi, Allan H. MacDonald, Jie Shan, and Kin Fai Mak, “Simulation of hubbard model physics in wse₂/ws₂ moiré superlattices,” *Nature* **579**, 353–358 (2020).
 - [18] Yang Xu, Song Liu, Daniel A Rhodes, Kenji Watanabe, Takashi Taniguchi, James Hone, Veit Elser, Kin Fai Mak, and Jie Shan, “Correlated insulating states at fractional fillings of moiré superlattices,” *Nature* **587**, 214–218 (2020).
 - [19] Emma C Regan, Danqing Wang, Chenhao Jin, M Iqbal Bakti Utama, Beini Gao, Xin Wei, Sihan Zhao, Wenyu Zhao, Zuocheng Zhang, Kentaro Yumigeta, *et al.*, “Mott and generalized Wigner crystal states in WSe₂/WS₂ moiré superlattices,” *Nature* **579**, 359–363 (2020).
 - [20] Jiaqi Cai, Eric Anderson, Chong Wang, Xiaowei Zhang, Xiaoyu Liu, William Holtzmann, Yinong Zhang, Fengren Fan, Takashi Taniguchi, Kenji Watanabe, Ying Ran, Ting Cao, Liang Fu, Di Xiao, Wang Yao, and Xiaodong Xu, “Signatures of fractional quantum anomalous hall states in twisted mote₂,” *Nature* **622**, 63–68 (2023).
 - [21] Erfu Liu, Takashi Taniguchi, Kenji Watanabe, Nathaniel M Gabor, Yong-Tao Cui, and Chun Hung Lui, “Excitonic and valley-polarization signatures of fractional correlated electronic phases in a WSe₂/WS₂ moiré superlattice,” *Physical Review Letters* **127**, 037402 (2021).
 - [22] Dongxue Chen, Zhen Lian, Xiong Huang, Ying Su, Mina Rashetnia, Lei Ma, Li Yan, Mark Blei, Li Xiang, Takashi Taniguchi, Kenji Watanabe, Sefaattin Tongay, Dmitry Smirnov, Zenghui Wang, Chuanwei Zhang, Yong-Tao Cui, and Su-Fei Shi, “Excitonic insulator in a heterojunction moiré superlattice,” *Nature Physics* **18**, 1171–1176 (2022).
 - [23] Zuocheng Zhang, Emma C. Regan, Danqing Wang, Wenyu Zhao, Shaoxin Wang, Mohammed Sayyad, Kentaro Yumigeta, Kenji Watanabe, Takashi Taniguchi, Sefaattin Tongay, Michael Crommie, Alex Zettl, Michael P. Zaletel, and Feng Wang, “Correlated interlayer exciton insulator in heterostructures of monolayer wse2 and moiré ws₂/wse₂,” *Nature Physics* **18**, 1214–1220 (2022).
 - [24] Richen Xiong, Jacob H. Nie, Samuel L. Brantly, Patrick Hays, Renee Sailus, Kenji Watanabe, Takashi Taniguchi, Sefaattin Tongay, and Chenhao Jin, “Correlated insulator of excitons in wse₂/ws₂ moiré superlattices,” *Science (New York, N.Y.)* **380**, 860–864 (2023).
 - [25] Trithep Devakul, Valentin Cr@pel, Yang Zhang, and Liang Fu, “Magic in twisted transition metal dichalcogenide bilayers,” *Nature communications* **12**, 6730 (2021).
 - [26] Hongyi Yu, Xiaodong Cui, Xiaodong Xu, and Wang Yao, “Valley excitons in two-dimensional semiconductors,” *National Science Review* **2**, 57–70 (2015).
 - [27] Gang Wang, Alexey Chernikov, Mikhail M Glazov, Tony F Heinz, Xavier Marie, Thierry Amand, and Bernhard Urbaszek, “Colloquium: Excitons in atomically thin transition metal dichalcogenides,” *Reviews of Modern Physics* **90**, 021001 (2018).

- [28] Alexey Chernikov, Timothy C Berkelbach, Heather M Hill, Albert Rigosi, Yilei Li, Ozgur Burak Aslan, David R Reichman, Mark S Hybertsen, and Tony F Heinz, “Exciton binding energy and nonhydrogenic Rydberg series in monolayer WS_2 ,” *Physical Review Letters* **113**, 076802 (2014).
- [29] Keliang He, Nardeep Kumar, Liang Zhao, Zefang Wang, Kin Fai Mak, Hui Zhao, and Jie Shan, “Tightly bound excitons in monolayer WSe_2 ,” *Physical Review Letters* **113**, 026803 (2014).
- [30] Di Xiao, Gui-Bin Liu, Wanxiang Feng, Xiaodong Xu, and Wang Yao, “Coupled spin and valley physics in monolayers of MoS_2 and other group-VI dichalcogenides,” *Physical Review Letters* **108**, 196802 (2012).
- [31] Xiaodong Xu, Wang Yao, Di Xiao, and Tony F Heinz, “Spin and pseudospins in layered transition metal dichalcogenides,” *Nature Physics* **10**, 343–350 (2014).
- [32] Kin Fai Mak, Keliang He, Jie Shan, and Tony F Heinz, “Control of valley polarization in monolayer MoS_2 by optical helicity,” *Nature Nanotechnology* **7**, 494–498 (2012).
- [33] Hualing Zeng, Junfeng Dai, Wang Yao, Di Xiao, and Xiaodong Cui, “Valley polarization in MoS_2 monolayers by optical pumping,” *Nature Nanotechnology* **7**, 490–493 (2012).
- [34] Ashish Arora, Matthias Drüppel, Robert Schmidt, Thorsten Deilmann, Robert Schneider, Maciej R Molas, Philipp Marauhn, Steffen Michaelis de Vasconcelos, Marek Potemski, Michael Rohlfing, *et al.*, “Interlayer excitons in a bulk van der waals semiconductor,” *Nature communications* **8**, 1–6 (2017).
- [35] Zefang Wang, Yi-Hsin Chiu, Kevin Honz, Kin Fai Mak, and Jie Shan, “Electrical tuning of interlayer exciton gases in WSe_2 bilayers,” *Nano Letters* **18**, 137–143 (2018).
- [36] Jason Horng, Tineke Stroucken, Long Zhang, Eunice Y Paik, Hui Deng, and Stephan W Koch, “Observation of interlayer excitons in MoSe_2 single crystals,” *Physical Review B* **97**, 241404 (2018).
- [37] Nadine Leisgang, Shivangi Shree, Ioannis Paradisanos, Lukas Sponfeldner, Cedric Robert, Delphine Lagarde, Andrea Balocchi, Kenji Watanabe, Takashi Taniguchi, Xavier Marie, *et al.*, “Giant Stark splitting of an exciton in bilayer MoS_2 ,” *Nature Nanotechnology* **15**, 901–907 (2020).
- [38] Etienne Lorchat, Malte Selig, Florian Katsch, Kentaro Yumigeta, Sefaattin Tongay, Andreas Knorr, Christian Schneider, and Sven Höfling, “Excitons in Bilayer MoS_2 Displaying a Colossal Electric Field Splitting and Tunable Magnetic Response,” *Physical Review Letters* **126**, 037401 (2021).
- [39] Namphung Peimyoo, Thorsten Deilmann, Freddie Withers, Janire Escolar, Darren Nutting, Takashi Taniguchi, Kenji Watanabe, Alireza Taghizadeh, Monica Felicia Craciun, Kristian Sommer Thygesen, *et al.*, “Electrical tuning of optically active interlayer excitons in bilayer MoS_2 ,” *Nature Nanotechnology* , 1–6 (2021).
- [40] Ioannis Paradisanos, Shivangi Shree, Antony George, Nadine Leisgang, Cedric Robert, Kenji Watanabe, Takashi Taniguchi, Richard J Warburton, Andrey Turchanin, Xavier Marie, *et al.*, “Controlling interlayer excitons in MoS_2 layers grown by chemical vapor deposition,” *Nature Communications* **11**, 1–7 (2020).
- [41] Jing Liang, Dongyang Yang, Jingda Wu, Jerry I Dadap, Kenji Watanabe, Takashi Taniguchi, and Ziliang Ye, “Optically probing the asymmetric interlayer coupling in rhombohedral-stacked mos_2 bilayer,” *Physical Review X* **12**, 041005 (2022).
- [42] Iann C Gerber, Emmanuel Courtade, Shivangi Shree, Cedric Robert, Takashi Taniguchi, Kenji Watanabe, Andrea Balocchi, Pierre Renucci, Delphine Lagarde, Xavier Marie, *et al.*, “Interlayer excitons in bilayer MoS_2 with strong oscillator strength up to room temperature,” *Physical Review B* **99**, 035443 (2019).
- [43] Shun Feng, Aidan Campbell, Mauro Brotons-Gisbert, Daniel Andres-Penares, Hyeonjun Baek, Takashi Taniguchi, Kenji Watanabe, Bernhard Urbaszek, Iann C Gerber, and Brian D Gerardot, “Highly Tunable Ground and Excited State Excitonic Dipoles in Multilayer 2H-MoSe_2 ,” arXiv preprint arXiv:2212.14338 (2022).
- [44] Yinong Zhang, Chengxin Xiao, Dmitry Ovchinnikov, Jiayi Zhu, Xi Wang, Takashi Taniguchi, Kenji Watanabe, Jiaqiang Yan, Wang Yao, and Xiaodong Xu, “Every-other-layer dipolar excitons in a spin-valley locked superlattice,” *Nature nanotechnology* **18**, 501–506 (2023).
- [45] Jun Kang, Sefaattin Tongay, Jian Zhou, Jingbo Li, and Junqiao Wu, “Band offsets and heterostructures of two-dimensional semiconductors,” *Applied Physics Letters* **102**, 012111 (2013).
- [46] Ming-Hui Chiu, Chendong Zhang, Hung-Wei Shiu, Chih-Piao Chuu, Chang-Hsiao Chen, Chih-Yuan S Chang, Chia-Hao Chen, Mei-Yin Chou, Chih-Kang Shih, and Lain-Jong Li, “Determination of band alignment in the single-layer $\text{MoS}_2/\text{WSe}_2$ heterojunction,” *Nature Communications* **6**, 7666 (2015).
- [47] Neil R Wilson, Paul V Nguyen, Kyle Seyler, Pasqual Rivera, Alexander J Marsden, Zachary PL Laker, Gabriel C Constantinescu, Viktor Kandyba, Alexei Barinov, Nicholas DM Hine, Xiaodong Xu, and David H Cobden, “Determination of band offsets, hybridization, and exciton binding in 2D semiconductor heterostructures,” *Science Advances* **3**, e1601832 (2017).
- [48] Pasqual Rivera, John R Schaibley, Aaron M Jones, Jason S Ross, Sanfeng Wu, Grant Aivazian, Philip Klement, Kyle Seyler, Genevieve Clark, Nirmal J Ghimire, Jiaqiang Yan, D. G. Mandrus, Wang Yao, and Xiaodong Xu, “Observation of long-lived interlayer excitons in monolayer MoSe_2 - WSe_2 heterostructures,” *Nature Communications* **6**, 6242 (2015).
- [49] Pasqual Rivera, Kyle L Seyler, Hongyi Yu, John R Schaibley, Jiaqiang Yan, David G Mandrus, Wang Yao, and Xiaodong Xu, “Valley-polarized exciton dynamics in a 2D semiconductor heterostructure,” *Science* **351**, 688–691 (2016).
- [50] Aubrey T Hanbicki, Hsun-Jen Chuang, Matthew R Rosenberger, C Stephen Hellberg, Saujan V Sivaram, Kathleen M McCreary, Igor I Mazin, and Berend T Jonker, “Double indirect interlayer exciton in a $\text{MoSe}_2/\text{WSe}_2$ van der Waals heterostructure,” *Acs Nano* **12**, 4719–4726 (2018).
- [51] Bastian Miller, Alexander Steinhoff, Borja Pano, Julian Klein, Frank Jahnke, Alexander Holleitner, and Ursula Wurstbauer, “Long-lived direct and indirect interlayer excitons in van der waals heterostructures,” *Nano Letters* **17**, 5229–5237 (2017).

- [52] Philipp Nagler, Gerd Plechinger, Mariana V Ballottin, Anatolie Mitioglu, Sebastian Meier, Nicola Paradiso, Christoph Strunk, Alexey Chernikov, Peter C M Christianen, Christian Schüller, and Tobias Korn, “Interlayer exciton dynamics in a dichalcogenide monolayer heterostructure,” *2D Materials* **4**, 025112 (2017).
- [53] Luis A Jauregui, Andrew Y Joe, Kateryna Pistunova, Dominik S Wild, Alexander A High, You Zhou, Giovanni Scuri, Kristiaan De Greve, Andrey Sushko, Che-Hang Yu, *et al.*, “Electrical control of interlayer exciton dynamics in atomically thin heterostructures,” *Science* **366**, 870–875 (2019).
- [54] Artur Branny, Santosh Kumar, Raphaël Proux, and Brian D Gerardot, “Deterministic strain-induced arrays of quantum emitters in a two-dimensional semiconductor,” *Nature Communications* **8**, 15053 (2017).
- [55] Carmen Palacios-Berraquero, Dhiren M Kara, Alejandro R-P Montblanch, Matteo Barbone, Pawel Latawiec, Duhee Yoon, Anna K Ott, Marko Loncar, Andrea C Ferrari, and Mete Atatüre, “Large-scale quantum-emitter arrays in atomically thin semiconductors,” *Nature Communications* **8**, 15093 (2017).
- [56] Malte Kremser, Mauro Brotons-Gisbert, Johannes Knörzer, Janine Gückelhorn, Moritz Meyer, Matteo Barbone, Andreas V Stier, Brian D Gerardot, Kai Müller, and Jonathan J Finley, “Discrete interactions between a few interlayer excitons trapped at a MoSe₂-WSe₂ heterointerface,” *npj 2D Materials and Applications* **4**, 1–6 (2020).
- [57] Weijie Li, Xin Lu, Sudipta Dubey, Luka Devenica, and Ajit Srivastava, “Dipolar interactions between localized interlayer excitons in van der Waals heterostructures,” *Nature Materials* **19**, 624 (2020).
- [58] Hongyi Yu, Gui-Bin Liu, Jianju Tang, Xiaodong Xu, and Wang Yao, “Moiré excitons: From programmable quantum emitter arrays to spin-orbit-coupled artificial lattices,” *Science Advances* **3**, e1701696 (2017).
- [59] Fengcheng Wu, Timothy Lovorn, and AH MacDonald, “Theory of optical absorption by interlayer excitons in transition metal dichalcogenide heterobilayers,” *Physical Review B* **97**, 035306 (2018).
- [60] Chendong Zhang, Chih-Piao Chuu, Xibiao Ren, Ming-Yang Li, Lain-Jong Li, Chuanhong Jin, Mei-Yin Chou, and Chih-Kang Shih, “Interlayer couplings, Moiré patterns, and 2D electronic superlattices in MoS₂/WSe₂ hetero-bilayers,” *Science Advances* **3**, e1601459 (2017).
- [61] Thorsten Deilmann, Michael Rohlfing, and Ursula Wurstbauer, “Light-matter interaction in van der waals hetero-structures,” *Journal of Physics: Condensed Matter* **32**, 333002 (2020).
- [62] Hongyi Yu, Gui-Bin Liu, and Wang Yao, “Brightened spin-triplet interlayer excitons and optical selection rules in van der Waals heterobilayers,” *2D Materials* **5**, 035021 (2018).
- [63] Kyle L Seyler, Pasqual Rivera, Hongyi Yu, Nathan P Wilson, Essance L Ray, David G Mandrus, Jiaqiang Yan, Wang Yao, and Xiaodong Xu, “Signatures of moiré-trapped valley excitons in MoSe₂/WSe₂ heterobilayers,” *Nature* **567**, 66–70 (2019).
- [64] Mauro Brotons-Gisbert, Hyeonjun Baek, Alejandro Molina-Sánchez, Aidan Campbell, Eleanor Scerri, Daniel White, Kenji Watanabe, Takashi Taniguchi, Cristian Bonato, and Brian D Gerardot, “Spin-layer locking of interlayer excitons trapped in moiré potentials,” *Nature Materials* **19**, 630 (2020).
- [65] Elyse Barré, Ouri Karni, Erfu Liu, Aidan L O’Beirne, Xueqi Chen, Henrique B Ribeiro, Leo Yu, Bumho Kim, Kenji Watanabe, Takashi Taniguchi, *et al.*, “Optical absorption of interlayer excitons in transition-metal dichalcogenide heterostructures,” *Science* **376**, 406–410 (2022).
- [66] Xi Wang, Jiayi Zhu, Kyle L. Seyler, Pasqual Rivera, Huiyuan Zheng, Yingqi Wang, Minhao He, Takashi Taniguchi, Kenji Watanabe, Jiaqiang Yan, David G. Mandrus, Daniel R. Gamelin, Wang Yao, and Xiaodong Xu, “Moiré trions in mose2/wse2 heterobilayers,” *Nature Nanotechnology* **16**, 1208–1213 (2021).
- [67] Erfu Liu, Elyse Barré, Jeremiah van Baren, Matthew Wilson, Takashi Taniguchi, Kenji Watanabe, Yong-Tao Cui, Nathaniel M Gabor, Tony F Heinz, Yia-Chung Chang, *et al.*, “Signatures of moiré trions in WSe₂/MoSe₂ heterobilayers,” *Nature* **594**, 46–50 (2021).
- [68] Hyeonjun Baek, Mauro Brotons-Gisbert, Aidan Campbell, Valerio Vitale, Johannes Lischner, Kenji Watanabe, Takashi Taniguchi, and Brian D Gerardot, “Optical read-out of Coulomb staircases in a moiré superlattice via trapped interlayer trions,” *Nature Nanotechnology* , 1–7 (2021).
- [69] Mauro Brotons-Gisbert, Hyeonjun Baek, Aidan Campbell, Kenji Watanabe, Takashi Taniguchi, and Brian D Gerardot, “Moiré-trapped interlayer trions in a charge-tunable WSe₂/MoSe₂ heterobilayer,” *Physical Review X* **11**, 1–12 (2021).
- [70] Tianmeng Wang, Shengnan Miao, Zhipeng Li, Yuze Meng, Zhengguang Lu, Zhen Lian, Mark Blei, Takashi Taniguchi, Kenji Watanabe, Sefaattin Tongay, *et al.*, “Giant valley-Zeeman splitting from spin-singlet and spin-triplet interlayer excitons in WSe₂/MoSe₂ heterostructure,” *Nano letters* **20**, 694–700 (2019).
- [71] Andrew Y Joe, Luis A Jauregui, Kateryna Pistunova, Andrés M Mier Valdivia, Zhengguang Lu, Dominik S Wild, Giovanni Scuri, Kristiaan De Greve, Ryan J Gelly, You Zhou, *et al.*, “Electrically controlled emission from singlet and triplet exciton species in atomically thin light-emitting diodes,” *Physical Review B* **103**, L161411 (2021).
- [72] Dinh Van Tuan, Su-Fei Shi, Xiaodong Xu, Scott A Crooker, and Hanan Dery, “Six-body and eight-body exciton states in monolayer WSe₂,” *Physical Review Letters* **129**, 076801 (2022).
- [73] Yuya Shimazaki, Clemens Kuhlenskamp, Ido Schwartz, Tomasz Smoleński, Kenji Watanabe, Takashi Taniguchi, Martin Kroner, Richard Schmidt, Michael Knap, and Ataç Imamoğlu, “Optical signatures of periodic charge distribution in a mott-like correlated insulator state,” *Physical Review X* **11**, 021027 (2021).
- [74] Chenhao Jin, Emma C Regan, Aiming Yan, M Iqbal Bakti Utama, Danqing Wang, Sihan Zhao, Ying Qin, Sijie Yang, Zhiren Zheng, Shenyang Shi, *et al.*, “Observation of moiré excitons in WSe₂/WS₂ heterostructure superlattices,” *Nature* **567**, 76 (2019).
- [75] David A. Ruiz-Tijerina and Vladimir I. Fal’ko, “Interlayer hybridization and moiré superlattice minibands for electrons and excitons in heterobilayers of transition-metal dichalcogenides,” *Phys. Rev. B* **99**, 125424 (2019).

- [76] Evgeny M Alexeev, David A Ruiz-Tijerina, Mark Danovich, Matthew J Hamer, Daniel J Terry, Pramoda K Nayak, Seongjoon Ahn, Sangyeon Pak, Juwon Lee, Jung Inn Sohn, *et al.*, “Resonantly hybridized excitons in moiré superlattices in van der Waals heterostructures,” *Nature* **567**, 81 (2019).
- [77] Fengcheng Wu, Timothy Lovorn, and Allan H MacDonald, “Topological exciton bands in moiré heterojunctions,” *Physical Review Letters* **118**, 147401 (2017).
- [78] Dongxue Chen, Zhen Lian, Xiong Huang, Ying Su, Mina Rashetnia, Li Yan, Mark Blei, Takashi Taniguchi, Kenji Watanabe, Sefaattin Tongay, *et al.*, “Tuning moiré excitons and correlated electronic states through layer degree of freedom,” *Nature Communications* **13**, 4810 (2022).
- [79] Mit H Naik, Emma C Regan, Zuocheng Zhang, Yang-Hao Chan, Zhenglu Li, Danqing Wang, Yoseob Yoon, Chin Shen Ong, Wenyu Zhao, Sihao Zhao, *et al.*, “Intralayer charge-transfer moiré excitons in van der waals superlattices,” *Nature* **609**, 52–57 (2022).
- [80] Xi Wang, Xiaowei Zhang, Jiayi Zhu, Heonjoon Park, Yingqi Wang, Chong Wang, William G Holtzmann, Takashi Taniguchi, Kenji Watanabe, Jiaqiang Yan, *et al.*, “Intercell moiré exciton complexes in electron lattices,” *Nature Materials* **22**, 599–604 (2023).
- [81] Jiho Sung, You Zhou, Giovanni Scuri, Viktor Zólyomi, Trond I Andersen, Hyobin Yoo, Dominik S Wild, Andrew Y Joe, Ryan J Gelly, Hoseok Heo, *et al.*, “Broken mirror symmetry in excitonic response of reconstructed domains in twisted $\text{mose}_2/\text{mose}_2$ bilayers,” *Nature Nanotechnology* **15**, 750–754 (2020).
- [82] Yanhao Tang, Jie Gu, Song Liu, Kenji Watanabe, Takashi Taniguchi, James Hone, Kin Fai Mak, and Jie Shan, “Tuning layer-hybridized moiré excitons by the quantum-confined Stark effect,” *Nature Nanotechnology* **16**, 52–57 (2021).
- [83] Yuya Shimazaki, Ido Schwartz, Kenji Watanabe, Takashi Taniguchi, Martin Kroner, and Ataç Imamoğlu, “Strongly correlated electrons and hybrid excitons in a moiré heterostructure,” *Nature* **580**, 472–477 (2020).
- [84] Philipp Nagler, Fabian Mooshammer, Jens Kunstmann, Mariana V Ballottin, Anatolie Mitioglu, Alexey Chernikov, Andrey Chaves, Frederick Stein, Nicola Paradiso, Sebastian Meier, *et al.*, “Interlayer excitons in transition-metal dichalcogenide heterobilayers,” *Physica Status Solidi (b)* **256**, 1900308 (2019).
- [85] Ke Wu, Hongxia Zhong, Quanbing Guo, Jibo Tang, Jing Zhang, Lihua Qian, Zhifeng Shi, Chendong Zhang, Shengjun Yuan, Shunping Zhang, *et al.*, “Identification of twist-angle-dependent excitons in WS_2/WSe_2 heterobilayers,” *National Science Review* (2021).
- [86] Lukas Sponfeldner, Nadine Leisgang, Shivangi Shree, Ioannis Paradisanos, Kenji Watanabe, Takashi Taniguchi, Cedric Robert, Delphine Lagarde, Andrea Balocchi, Xavier Marie, *et al.*, “Capacitively-coupled and inductively-coupled excitons in bilayer MoS_2 ,” arXiv preprint arXiv:2108.04248 (2021).
- [87] Borislav Polovnikov, Johannes Scherzer, Subhadeep Misra, Xin Huang, Christian Mohl, Zhijie Li, Jonas Göser, Jonathan Förste, Ismail Bilgin, Kenji Watanabe, Takashi Taniguchi, Alexander Högele, and Anvar S. Baimuratov, “Field-Induced Hybridization of Moiré Excitons in M_2/WS_2 Heterobilayers,” *Phys. Rev. Lett.* **132**, 076902 (2024).
- [88] Yusong Bai, Lin Zhou, Jue Wang, Wenjing Wu, Leo J McGilly, Dorri Halbertal, Chiu Fan Bowen Lo, Fang Liu, Jenny Ardelean, Pasqual Rivera, *et al.*, “Excitons in strain-induced one-dimensional moiré potentials at transition metal dichalcogenide heterojunctions,” *Nature Materials* **19**, 1068–1073 (2020).
- [89] Shen Zhao, Zhijie Li, Xin Huang, Anna Rupp, Jonas Göser, Ilia A. Vovk, Stanislav Yu. Kruchinin, Kenji Watanabe, Takashi Taniguchi, Ismail Bilgin, Anvar S. Baimuratov, and Alexander Högele, “Excitons in mesoscopically reconstructed moiré heterostructures,” *Nature Nanotechnology* **18**, 572–579 (2023).
- [90] Zhijie Li, Farsane Tabataba-Vakili, Shen Zhao, Anna Rupp, Ismail Bilgin, Ziria Herdegen, Benjamin März, Kenji Watanabe, Takashi Taniguchi, Gabriel Ravanhani Schleder, Anvar S. Baimuratov, Efthimios Kaxiras, Knut Müller-Caspary, and Alexander Högele, “Lattice reconstruction in $\text{mose}_2\text{-wse}_2$ heterobilayers synthesized by chemical vapor deposition,” *Nano Letters* **23**, 4160–4166 (2023), PMID: 37141148, <https://doi.org/10.1021/acs.nanolett.2c05094>.
- [91] VV Enaldiev, Viktor Zólyomi, CELAL Yelgel, SJ Magorrian, and VI Fal’ko, “Stacking domains and dislocation networks in marginally twisted bilayers of transition metal dichalcogenides,” *Physical Review Letters* **124**, 206101 (2020).
- [92] Astrid Weston, Yichao Zou, Vladimir Enaldiev, Alex Summerfield, Nicholas Clark, Viktor Zólyomi, Abigail Graham, Celal Yelgel, Samuel Magorrian, Mingwei Zhou, *et al.*, “Atomic reconstruction in twisted bilayers of transition metal dichalcogenides,” *Nature Nanotechnology* **15**, 592–597 (2020).
- [93] Leo J McGilly, Alexander Kerelsky, Nathan R Finney, Konstantin Shapovalov, En-Min Shih, Augusto Ghiotto, Yihang Zeng, Samuel L Moore, Wenjing Wu, Yusong Bai, *et al.*, “Visualization of moiré superlattices,” *Nature Nanotechnology* **15**, 580–584 (2020).
- [94] Matthew R Rosenberger, Hsun-Jen Chuang, Madeleine Phillips, Vladimir P Oleshko, Kathleen M McCreary, Saujan V Sivaram, C Stephen Hellberg, and Berend T Jonker, “Twist angle-dependent atomic reconstruction and moiré patterns in transition metal dichalcogenide heterostructures,” *ACS Nano* **14**, 4550–4558 (2020).
- [95] Trond I. Andersen, Giovanni Scuri, Andrey Sushko, Kristiaan de Greve, Jiho Sung, You Zhou, Dominik S. Wild, Ryan J. Gelly, Hoseok Heo, Damien Bérubé, Andrew Y. Joe, Luis A. Jauregui, Kenji Watanabe, Takashi Taniguchi, Philip Kim, Hongkun Park, and Mikhail D. Lukin, “Excitons in a reconstructed moiré potential in twisted $\text{wse}_2/\text{wse}_2$ homobilayers,” *Nature materials* **20**, 480–487 (2021).
- [96] Shen Zhao, Zhijie Li, Xin Huang, Anna Rupp, Jonas Göser, Ilia A. Vovk, Stanislav Yu. Kruchinin, Kenji Watanabe, Takashi Taniguchi, Ismail Bilgin, Anvar S. Baimuratov, and Alexander Högele, “Excitons in mesoscopically reconstructed moiré heterostructures,” *Nature Nanotechnology* **18**, 572–579 (2023).
- [97] Ligu Ma, Phuong X. Nguyen, Zefang Wang, Yongxin Zeng, Kenji Watanabe, Takashi Taniguchi, Allan H. MacDonald, Kin Fai Mak, and Jie Shan, “Strongly correlated excitonic insulator in atomic double layers,” *Nature* **598**, 585–589 (2021).

- [98] Heonjoon Park, Jiayi Zhu, Xi Wang, Yingqi Wang, William Holtzmann, Takashi Taniguchi, Kenji Watanabe, Jiaqiang Yan, Liang Fu, Ting Cao, Di Xiao, Daniel R. Gamelin, Hongyi Yu, Wang Yao, and Xiaodong Xu, “Dipole ladders with large hubbard interaction in a moiré exciton lattice,” *Nature Physics* **19**, 1286–1292 (2023).
- [99] Fengcheng Wu, Timothy Lovorn, Emanuel Tutuc, and Allan H MacDonald, “Hubbard model physics in transition metal dichalcogenide moiré bands,” *Physical review letters* **121**, 026402 (2018).
- [100] Mit H Naik and Manish Jain, “Ultraflatbands and shear solitons in moiré patterns of twisted bilayer transition metal dichalcogenides,” *Physical Review Letters* **121**, 266401 (2018).
- [101] Yanhao Tang, Lizhong Li, Tingxin Li, Yang Xu, Song Liu, Katayun Barmak, Kenji Watanabe, Takashi Taniguchi, Allan H MacDonald, Jie Shan, *et al.*, “Simulation of hubbard model physics in wse₂/ws₂ moiré superlattices,” *Nature* **579**, 353–358 (2020).
- [102] A. H. MacDonald, “Introduction to the physics of the quantum hall regime,” arXiv:cond-mat/9410047 (1994), doi.org/10.48550/arXiv.cond-mat/9410047.
- [103] John M. Blatt, K. W. Böer, and Werner Brandt, “Bose-Einstein Condensation of Excitons,” *Physical Review* **126**, 1691–1692 (1962), publisher: American Physical Society.
- [104] B. Laikhtman and R. Rapaport, “Exciton correlations in coupled quantum wells and their luminescence blue shift,” *Physical Review B* **80**, 195313 (2009), publisher: American Physical Society.
- [105] M. M. Fogler, L. V. Butov, and K. S. Novoselov, “High-temperature superfluidity with indirect excitons in van der Waals heterostructures,” *Nature Communications* **5**, 4555 (2014), number: 1 Publisher: Nature Publishing Group.
- [106] Manuel Katzer, Malte Selig, Lukas Sigl, Mirco Troue, Johannes Figueiredo, Jonas Kiemle, Florian Sigger, Ursula Wurstbauer, Alexander W. Holleitner, and Andreas Knorr, “Exciton-phonon scattering: Competition between the bosonic and fermionic nature of bound electron-hole pairs,” *Physical Review B* **108**, L121102 (2023), publisher: American Physical Society.
- [107] Mirco Troue, Johannes Figueiredo, Lukas Sigl, Christos Paspalides, Manuel Katzer, Takashi Taniguchi, Kenji Watanabe, Malte Selig, Andreas Knorr, Ursula Wurstbauer, and Alexander W. Holleitner, “Extended Spatial Coherence of Interlayer Excitons in $\{\mathrm{MoSe}\}_2/\{\mathrm{WSe}\}_2$ Heterobilayers,” *Physical Review Letters* **131**, 036902 (2023), publisher: American Physical Society.
- [108] J. P. Eisenstein and A. H. MacDonald, “Bose–Einstein condensation of excitons in bilayer electron systems,” *Nature* **432**, 691–694 (2004), number: 7018 Publisher: Nature Publishing Group.
- [109] Michael Stern, Vladimir Umansky, and Israel Bar-Joseph, “Exciton Liquid in Coupled Quantum Wells,” *Science* **343**, 55–57 (2014), publisher: American Association for the Advancement of Science.
- [110] Xiaomeng Liu, Kenji Watanabe, Takashi Taniguchi, Bertrand I. Halperin, and Philip Kim, “Quantum Hall drag of exciton condensate in graphene,” *Nature Physics* **13**, 746–750 (2017), number: 8 Publisher: Nature Publishing Group.
- [111] Zefang Wang, Daniel A. Rhodes, Kenji Watanabe, Takashi Taniguchi, James C. Hone, Jie Shan, and Kin Fai Mak, “Evidence of high-temperature exciton condensation in two-dimensional atomic double layers,” *Nature* **574**, 76–80 (2019), number: 7776 Publisher: Nature Publishing Group.
- [112] Anshul Kogar, Melinda S. Rak, Sean Vig, Ali A. Husain, Felix Flicker, Young Il Joe, Luc Venema, Greg J. MacDougall, Tai C. Chiang, Eduardo Fradkin, Jasper van Wezel, and Peter Abbamonte, “Signatures of exciton condensation in a transition metal dichalcogenide,” *Science* **358**, 1314–1317 (2017), publisher: American Association for the Advancement of Science.
- [113] Mathieu Alloing, Mussie Beian, Maciej Lewenstein, David Fuster, Yolanda González, Luisa González, Roland Combescot, Monique Combescot, and François Dubin, “Evidence for a Bose-Einstein condensate of excitons,” *Europhysics Letters* **107**, 10012 (2014), publisher: EDP Sciences, IOP Publishing and Società Italiana di Fisica.
- [114] A. A. High, J. R. Leonard, M. Remeika, L. V. Butov, M. Hanson, and A. C. Gossard, “Condensation of Excitons in a Trap,” *Nano Letters* **12**, 2605–2609 (2012), publisher: American Chemical Society.
- [115] A. Griffin, D. W. Snoke, and S. Stringari, “Bose-Einstein Condensation,” (1995), iSBN: 9780521464734 9780521589901 9780511524240 Publisher: Cambridge University Press.
- [116] Aubrey T. Hanbicki, Hsun-Jen Chuang, Matthew R. Rosenberger, C. Stephen Hellberg, Saujan V. Sivaram, Kathleen M. McCreary, Igor I. Mazin, and Berend T. Jonker, “Double Indirect Interlayer Exciton in a MoSe₂/WSe₂ van der Waals Heterostructure,” *ACS Nano* **12**, 4719–4726 (2018), publisher: American Chemical Society.
- [117] P. Merkl, F. Mooshammer, P. Steinleitner, A. Girnguber, K.-Q. Lin, P. Nagler, J. Holler, C. Schüller, J. M. Lupton, T. Korn, S. Ovesen, S. Brem, E. Malic, and R. Huber, “Ultrafast transition between exciton phases in van der Waals heterostructures,” *Nature Materials* **18**, 691–696 (2019), number: 7 Publisher: Nature Publishing Group.
- [118] L. V. Butov, A. A. Shashkin, V. T. Dolgoplov, K. L. Campman, and A. C. Gossard, “Magneto-optics of the spatially separated electron and hole layers in gaas/alxgal-xas coupled quantum wells,” *Physical Review B* **60**, 8753–8758 (1999), publisher: American Physical Society.
- [119] Z. Vörös, R. Balili, D. W. Snoke, L. Pfeiffer, and K. West, “Long-Distance Diffusion of Excitons in Double Quantum Well Structures,” *Physical Review Letters* **94**, 226401 (2005), publisher: American Physical Society.
- [120] A. Gärtner, A. W. Holleitner, J. P. Kotthaus, and D. Schuh, “Drift mobility of long-living excitons in coupled GaAs quantum wells,” *Applied Physics Letters* **89**, 052108 (2006).
- [121] A. Gärtner, L. Prectel, D. Schuh, A. W. Holleitner, and J. P. Kotthaus, “Micropatterned electrostatic traps for indirect excitons in coupled GaAs quantum wells,” *Physical Review B* **76**, 085304 (2007), publisher: American Physical Society.
- [122] X. P. Vögele, D. Schuh, W. Wegscheider, J. P. Kotthaus, and A. W. Holleitner, “Density Enhanced Diffusion of

- Dipolar Excitons within a One-Dimensional Channel,” *Physical Review Letters* **103**, 126402 (2009), publisher: American Physical Society.
- [123] Roland Zimmermann and Christoph Schindler, “Exciton–exciton interaction in coupled quantum wells,” *Solid State Communications Spontaneous coherence in exciton systems*, **144**, 395–398 (2007).
- [124] M. M. Glazov, “Phonon wind and drag of excitons in monolayer semiconductors,” *Physical Review B* **100**, 045426 (2019), publisher: American Physical Society.
- [125] Koloman Wagner, Jonas Zipfel, Roberto Rosati, Edith Wietek, Jonas D. Ziegler, Samuel Brem, Raúl Perea-Causín, Takashi Taniguchi, Kenji Watanabe, Mikhail M. Glazov, Ermin Malic, and Alexey Chernikov, “Nonclassical Exciton Diffusion in Monolayer $\{\mathrm{WSe}\}_2$,” *Physical Review Letters* **127**, 076801 (2021), publisher: American Physical Society.
- [126] Zhe Sun, Alberto Ciarrocchi, Fedele Tagarelli, Juan Francisco Gonzalez Marin, Kenji Watanabe, Takashi Taniguchi, and Andras Kis, “Excitonic transport driven by repulsive dipolar interaction in a van der waals heterostructure,” *Nature Photonics*, 1–7 (2021).
- [127] Kanak Datta, Zhengyang Lyu, Zidong Li, Takashi Taniguchi, Kenji Watanabe, and Parag B. Deotare, “Spatiotemporally controlled room-temperature exciton transport under dynamic strain,” *Nature Photonics* **16**, 242–247 (2022), number: 3 Publisher: Nature Publishing Group.
- [128] Ruoming Peng, Adina Ripin, Yusen Ye, Jiayi Zhu, Changming Wu, Seokhyeong Lee, Huan Li, Takashi Taniguchi, Kenji Watanabe, Ting Cao, Xiaodong Xu, and Mo Li, “Long-range transport of 2D excitons with acoustic waves,” *Nature Communications* **13**, 1334 (2022), number: 1 Publisher: Nature Publishing Group.
- [129] Malte Selig, Gunnar Berghäuser, Archana Raja, Philipp Nagler, Christian Schüller, Tony F. Heinz, Tobias Korn, Alexey Chernikov, Ermin Malic, and Andreas Knorr, “Excitonic linewidth and coherence lifetime in monolayer transition metal dichalcogenides,” *Nature Communications* **7** (2016), 10.1038/ncomms13279.
- [130] Galan Moody, Chandriker Kavir Dass, Kai Hao, Chang-Hsiao Chen, Lain-Jong Li, Akshay Singh, Kha Tran, Genevieve Clark, Xiaodong Xu, Gunnar Berghäuser, Ermin Malic, Andreas Knorr, and Xiaoqin Li, “Intrinsic homogeneous linewidth and broadening mechanisms of excitons in monolayer transition metal dichalcogenides,” *Nature Communications* **6**, 1–6 (2015).
- [131] Rodney Loudon, *The Quantum Theory of Light*, 3rd ed. (Oxford University Press, Oxford, 2000).
- [132] S. Savasta, O. Di Stefano, V. Savona, and W. Langbein, “Quantum Complementarity of Microcavity Polaritons,” *Physical Review Letters* **94**, 246401 (2005), publisher: American Physical Society.
- [133] Eunice Y. Paik, Long Zhang, G. William Burg, Rahul Gogna, Emanuel Tutuc, and Hui Deng, “Interlayer exciton laser of extended spatial coherence in atomically thin heterostructures,” *Nature* **576**, 80–84 (2019), number: 7785 Publisher: Nature Publishing Group.
- [134] G. J. Schinner, J. Repp, E. Schubert, A. K. Rai, D. Reuter, A. D. Wieck, A. O. Govorov, A. W. Holleitner, and J. P. Kotthaus, “Confinement and Interaction of Single Indirect Excitons in a Voltage-Controlled Trap Formed Inside Double InGaAs Quantum Wells,” *Physical Review Letters* **110**, 127403 (2013), publisher: American Physical Society.
- [135] Y. Y. Kuznetsova, P. Andreakou, M. W. Hasling, J. R. Leonard, E. V. Calman, L. V. Butov, M. Hanson, and A. C. Gossard, “Two-dimensional snowflake trap for indirect excitons,” *Optics Letters* **40**, 589 (2015).
- [136] Daniel N. Shanks, Fateme MahdikhanySarvejahany, Christine Muccianti, Adam Alfrey, Michael R. Koehler, David G. Mandrus, Takashi Taniguchi, Kenji Watanabe, Hongyi Yu, Brian J. LeRoy, and John R. Schaibley, “Nanoscale Trapping of Interlayer Excitons in a 2D Semiconductor Heterostructure,” *Nano Letters* **21**, 5641–5647 (2021), publisher: American Chemical Society.
- [137] Lukas Sigl, Mirco Troue, Manuel Katzer, Malte Selig, Florian Sigger, Jonas Kiemle, Mauro Brotons-Gisbert, Kenji Watanabe, Takashi Taniguchi, Brian D. Gerardot, Andreas Knorr, Ursula Wurstbauer, and Alexander W. Holleitner, “Optical dipole orientation of interlayer excitons in $\{\mathrm{MoSe}\}_2$ heterostacks,” *Physical Review B* **105**, 035417 (2022), publisher: American Physical Society.
- [138] Xiaoping Hong, Jonghwan Kim, Su-Fei Shi, Yu Zhang, Chenhao Jin, Yinghui Sun, Sefaattin Tongay, Junqiao Wu, Yanfeng Zhang, and Feng Wang, “Ultrafast charge transfer in atomically thin $\mathrm{mos}_2/\mathrm{ws}_2$ heterostructures,” *Nature Nanotechnology* **9**, 682–686 (2014).
- [139] Giuseppe Meneghini, Samuel Brem, and Ermin Malic, “Ultrafast phonon-driven charge transfer in van der waals heterostructures,” *Natural Sciences* **2** (2022), 10.1002/ntls.20220014.
- [140] Julien Madéo, Michael K. L. Man, Chakradhar Sahoo, Marshall Campbell, Vivek Pareek, E. Laine Wong, Abdullah Al-Mahboob, Nicholas S. Chan, Arka Karmakar, Bala Murali Krishna Mariserla, Xiaoqin Li, Tony F. Heinz, Ting Cao, and Keshav M. Dani, “Directly visualizing the momentum-forbidden dark excitons and their dynamics in atomically thin semiconductors,” *Science (New York, N.Y.)* **370**, 1199–1204 (2020).
- [141] Jonas E. Zimmermann, Marleen Axt, Fabian Mooshammer, Philipp Nagler, Christian Schüller, Tobias Korn, Ulrich Höfer, and Gerson Mette, “Ultrafast charge-transfer dynamics in twisted $\mathrm{mos}_2/\mathrm{wse}_2$ heterostructures,” *ACS nano* **15**, 14725–14731 (2021).
- [142] David Schmitt, Jan Philipp Bange, Wiebke Bennecke, AbdulAziz AlMutairi, Giuseppe Meneghini, Kenji Watanabe, Takashi Taniguchi, Daniel Steil, D. Russell Luke, R. Thomas Weitz, Sabine Steil, G. S. Matthijs Jansen, Samuel Brem, Ermin Malic, Stephan Hofmann, Marcel Reutzler, and Stefan Mathias, “Formation of moiré interlayer excitons in space and time,” *Nature* **608**, 499–503 (2022).
- [143] Jan Philipp Bange, Paul Werner, David Schmitt, Wiebke Bennecke, Giuseppe Meneghini, AbdulAziz Al-Mutairi, Marco Merboldt, Kenji Watanabe, Takashi Taniguchi, Sabine Steil, Daniel Steil, R. Thomas Weitz, Stephan Hofmann, G. S. Matthijs Jansen, Samuel Brem, Ermin Malic, Marcel Reutzler, and Stefan Mathias, “Ultrafast dynamics of bright and dark excitons in monolayer wse_2 and heterobilayer $\mathrm{wse}_2/\mathrm{mos}_2$,” *2D Materials* **10**, 035039 (2023).
- [144] Iris Niehues, Philipp Marauhn, Thorsten Deilmann, Daniel Wigger, Robert Schmidt, Ashish Arora, Stef-

- fen Michaelis de Vasconcellos, Michael Rohlfing, and Rudolf Bratschkis, "Strain tuning of the stokes shift in atomically thin semiconductors," *Nanoscale* **12**, 20786–20796 (2020).
- [145] Aditya Sood, Jonah B. Haber, Johan Carlström, Elizabeth A. Peterson, Elyse Barre, Johnathan D. Georgaras, Reid, Alexander H. M., Xiaozhe Shen, Marc E. Zajac, Emma C. Regan, Jie Yang, Takashi Taniguchi, Kenji Watanabe, Feng Wang, Xijie Wang, Jeffrey B. Neaton, Tony F. Heinz, Aaron M. Lindenberg, Felipe H. Da Jornada, and Archana Raja, "Bidirectional phonon emission in two-dimensional heterostructures triggered by ultrafast charge transfer," *Nature Nanotechnology* **18**, 29–35 (2023).
- [146] Ermin Malic, Raúl Perea-Causin, Roberto Rosati, Daniel Erckensten, and Samuel Brem, "Exciton transport in atomically thin semiconductors," *Nature communications* **14**, 3430 (2023).
- [147] Edith Wietek, Matthias Florian, Jonas Göser, Takashi Taniguchi, Kenji Watanabe, Alexander Högele, Mikhail M. Glazov, Alexander Steinhoff, and Alexey Chernikov, "Nonlinear and negative effective diffusivity of interlayer excitons in moiré-free heterobilayers," *Phys. Rev. Lett.* **132**, 016202 (2024).
- [148] Willy Knorr, Samuel Brem, Giuseppe Meneghini, and Ermin Malic, "Exciton transport in a moiré potential: From hopping to dispersive regime," *Physical Review Materials* **6** (2022), 10.1103/PhysRevMaterials.6.124002.
- [149] Junho Choi, Wei-Ting Hsu, Li-Syuan Lu, Liuyang Sun, Hui-Yu Cheng, Ming-Hao Lee, Jiamin Quan, Kha Tran, Chun-Yuan Wang, Matthew Staab, Kayleigh Jones, Takashi Taniguchi, Kenji Watanabe, Ming-Wen Chu, Shangjr Gwo, Suenne Kim, Chih-Kang Shih, Xiaoqin Li, and Wen-Hao Chang, "Moiré potential impedes interlayer exciton diffusion in van der waals heterostructures," *Science Advances* **6**, eaba8866 (2020), <https://www.science.org/doi/pdf/10.1126/sciadv.aba8866>.
- [150] Long Yuan, Biyuan Zheng, Jens Kunstmann, Thomas Brumme, Agnieszka Beata Kuc, Chao Ma, Shibin Deng, Daria Blach, Anlian Pan, and Libai Huang, "Twist-angle-dependent interlayer exciton diffusion in ws₂-wse₂ heterobilayers," *Nature materials* **19**, 617–623 (2020).
- [151] Zidong Li, Xiaobo Lu, Darwin F. Cordovilla Leon, Zhengyang Lyu, Hongchao Xie, Jize Hou, Yanzhao Lu, Xiaoyu Guo, Austin Kaczmarek, Takashi Taniguchi, Kenji Watanabe, Liuyan Zhao, Li Yang, and Parag B. Deotare, "Interlayer exciton transport in mose₂/wse₂ heterostructures," *ACS nano* **15**, 1539–1547 (2021).
- [152] Ke Wang, Kristiaan De Greve, Luis A Jauregui, Andrey Sushko, Alexander High, You Zhou, Giovanni Scuri, Takashi Taniguchi, Kenji Watanabe, Mikhail D Lukin, *et al.*, "Electrical control of charged carriers and excitons in atomically thin materials," *Nature Nanotechnology* **13**, 128–132 (2018).
- [153] Daniel N Shanks, Fateme MahdikhanySarvejahany, Christine Muccianti, Adam Alfrey, Michael R Koehler, David G Mandrus, Takashi Taniguchi, Kenji Watanabe, Hongyi Yu, Brian J LeRoy, *et al.*, "Nanoscale trapping of interlayer excitons in a 2d semiconductor heterostructure," *Nano Letters* **21**, 5641–5647 (2021).
- [154] Deepankur Thureja, Atac Imamoglu, Tomasz Smoleński, Ivan Amelio, Alexander Popert, Thibault Chervy, Xiaobo Lu, Song Liu, Katayun Barmak, Kenji Watanabe, *et al.*, "Electrically tunable quantum confinement of neutral excitons," *Nature* **606**, 298–304 (2022).
- [155] Yevgeny Slobodkin, Yotam Mazuz-Harpaz, Sivan Refaely-Abramson, Snir Gazit, Hadar Steinberg, and Ronen Rapaport, "Quantum phase transitions of trilayer excitons in atomically thin heterostructures," *Physical Review Letters* **125**, 255301 (2020).
- [156] Camille Lagoin and François Dubin, "Key role of the moiré potential for the quasicondensation of interlayer excitons in van der Waals heterostructures," *Physical Review B* **103**, L041406 (2021).
- [157] Daniel Erckensten, Samuel Brem, and Ermin Malic, "Exciton-exciton interaction in transition metal dichalcogenide monolayers and van der Waals heterostructures," *Physical Review B* **103**, 045426 (2021).
- [158] Jue Wang, Qianhui Shi, En-Min Shih, Lin Zhou, Wenjing Wu, Yusong Bai, Daniel Rhodes, Katayun Barmak, James Hone, Cory R Dean, *et al.*, "Diffusivity reveals three distinct phases of interlayer excitons in MoSe₂/WSe₂ heterobilayers," *Physical Review Letters* **126**, 106804 (2021).
- [159] Niclas Götzting, Frederik Lohof, and Christopher Gies, "Moiré-bose-hubbard model for interlayer excitons in twisted transition metal dichalcogenide heterostructures," *Physical Review B* **105**, 165419 (2022).
- [160] M. Kögl, P. Soubelet, M. Brotons-Gisbert, A. V. Stier, B. D. Gerardot, and J. J. Finley, "Moiré straintronics: a universal platform for reconfigurable quantum materials," *npj 2D Materials and Applications* **7** (2023), 10.1038/s41699-023-00382-4.
- [161] A. Inbar, J. Birkbeck, J. Xiao, T. Taniguchi, K. Watanabe, B. Yan, Y. Oreg, Ady Stern, E. Berg, and S. Ilani, "The quantum twisting microscope," *Nature* **614**, 682–687 (2023).